Squaramide-based supramolecular materials for 3D cell culture applications

Tong, C.

CHAPTER 3

On-demand light-activated stiffening of a multicomponent supramolecular material to direct cellular behavior in 3D

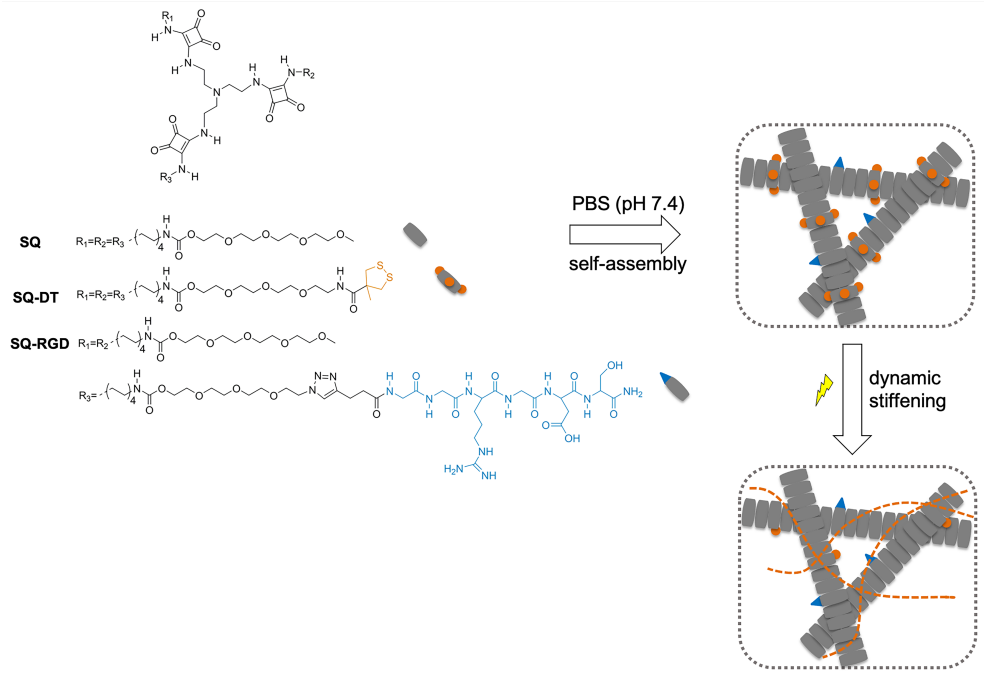

This chapter was prepared as an original research paper: Ciqing Tong, Joeri A. J. Wondergem, Markus C. Kwakernaak, Marco M. R. M. Hendrix, Ilja K. Voets, S. E. le Dévédec, Erik H. J. Danen, Doris Heinrich and Roxanne E. Kieltyka

3.1 Abstract

Supramolecular materials provide opportunities to mimic both the structural and dynamic aspects of native tissues. However, limited strategies exist to evolve their mechanical properties over time in the presence of cells as encountered in a range of developmental and disease processes. We herein disclose the design and synthesis of a squaramide-based tripodal supramolecular monomer functionalized with 1,2-dithiolane (DT) moieties. Through co-assembly with a native squaramide monomer, multicomponent supramolecular hydrogels with storage moduli in the range of ~200 Pa were obtained that could be stiffened to >10 kPa with UV light irradiation (365-375 nm) that triggers the opening of the 1,2-dithiolane ring to form disulfide crosslinks. Temporal control over hydrogel mechanical properties could be achieved through stepwise UV light irradiation. Cell adhesive cues (e.g., RGD peptide) could be spatially incorporated into the supramolecular network by applying a photomask or direct laser writing using UV light. Moreover, the effect of dynamic stiffening of the supramolecular polymer networks was readout using the change of the spread morphology of myoblast cells C2C12 and also the speed and persistence migration of breast cancer cells Hs578T.

3.2 Introduction

The natural extracellular matrix presents cues to cells in both space and time to direct cellular behavior over several length scales in development and disease.[1-5] For example, biophysical cues are known to change over time in several tissues (e.g., bone, brain and cardiovascular tissues) during the process of development.[6] However, current in vitro culture protocols largely recapitulate the dynamic presentation of biophysical cues from this natural material to direct cell fate in combination with biologically-derived materials (e.g., Matrigel, collagen).[7] Synthetic polymer materials have also been examined in this area because of their potential to overcome some of the challenges associated with natural materials, but are largely static, lacking the capacity to mimic the dynamic complexity encountered in natural tissues.[7] Past strategies to dynamically (or reversibly) soften and stiffen synthetic materials to influence cell behavior in 3D, have involved varying the ion concentration, pH, hydrogel composition, and UV light irradiation.[8-21] However, these strategies have been largely used in combination with covalent polymers, and sparingly in those that are supramolecular, but are essential to improve their approximation of the dynamic complexity, namely the spatiotemporal presentation of these biophysical cues, in native tissues.[22, 23]

Hierarchically self-assembled supramolecular materials are attractive for applications in the biomedical area because they show attractive properties such as tunability, responsiveness, mimicry of biopolymer network structure and mechanics, and modularity with precise control over the structural and molecular features of the monomers.[24-27] In these materials, small molecules are pre-encoded with non-covalent interactions that trigger their self-assembly into fibrillar aggregates and gel phase materials that can mechanically mimic features of natural biopolymer networks.[26] While the supramolecular nature of the assemblies endows these materials with reversible properties, their stiffness is often low limiting their broad applicability.[7] Post-modification of the aggregates through their covalent capture can be envisaged as a strategy to modulate mechanical properties of these materials, however, most modifications of such gelators result in gel-to-sol transitions and those that involve increasing gel stiffness remain rare, but critical for their biomedical application.[27, 28]

Bio-orthogonal strategies such as enzymatic reactions, irreversible click reactions and dynamic covalent crosslinks have been employed in covalent polymer materials to guide their mechanical properties enabling user-defined control.[29, 30] Of these strategies, disulfide crosslinking provides opportunities for

endowing dynamic character in these matrices due to their inherent reversible character that arises from the thiol-disulfide exchange reactions.[30] However, one limitation of free thiols is their high reactivity that causes the formation of disulfide bonds even on storage,[31] which can hinder the possibility for user-defined control. To this end, cyclic 1,2-dithiolanes have been used to modify polymers and fabricate dynamic hydrogel materials either through chemical reactions (e.g., free thiol induced ring opening polymerization)[32-34] or photo induced crosslinks[35, 36] in a controlled manner. More recently, we have demonstrated that such cyclic disulfides can be controlled spatiotemporally using UV light to engineer covalent polymer networks with dual covalent and reversible-covalent crosslinks for 3D cell culture applications.[37] However, the application of the cyclic 1,2-dithiolane unit for crosslinking of self-assembled molecular monomers for tissue engineering has not been considered, but can provide a powerful approach to tune the mechanical properties of such networks in a user-defined manner while opening possibilities to extend their mimicry of the dynamic mechanical processes that occur in native tissues.

We earlier reported a supramolecular polymer system based on squaramide-based monomers that form cytocompatible hydrogel materials. Squaramides are ditopic hydrogen bonding synthons[38-40] that have been demonstrated to self-assemble into supramolecular polymers in a head-to-tail hydrogen bonding arrangement when embedded within the hydrophobic domain of a monomer.[41-43] Soft, self-recovering materials were prepared that could be used to seed sensitive cell types such as induced pluripotent stem cells, however, the lack of bioactive cues (e.g., RGD peptide) and low modulus limit their application for a broad range of targets in 3D cell culture. We particularly became interested to introduce cyclic disulfides, namely 1,2-dithiolanes, into the squaramide monomers because of their ability to undergo ring opening polymerization, capacity to be triggered with light, small molecular size and biological relevance. We herein introduce 1,2-dithiolanes into a supramolecular polymer and evaluate its subsequent cross-linking through UV light irradiation (365 nm) to control the mechanical and bioactive properties of a hierarchically self-assembled matrix in space and time, which has not been reported yet.

3.3 Results and discussion

3.3.1 Synthesis of tripodal squaramide-based monomers SQ, SQ-DT and SQ-RGD

In order to facilitate the cross-linking of supramolecular monomers by the DT unit, the tripodal dithiolane based monomer **SQ-DT** (**Figure 3.1A**) was prepared by outfitting the **SQ** monomer with DT through an amide linkage. Using the maximum absorbance peak of 1,2-dithiolane (DT) at 330 nm, its ring opening was triggered by UV light (e.g., 365-375 nm) to initiate photo-crosslinking of the supramolecular polymer network and modulation of its gel properties. Moreover, a bioactive **SQ-RGD** monomer was also prepared where one arm of **SQ** was modified with an RGD peptide to facilitate integrin binding to the supramolecular material.

The native squaramide-based monomer (**SQ**) was synthesized as previously described.[43] The three-arm dithiolane functioned squaramide based monomer (**SQ-DT**) was synthesized as shown in **Scheme S3.1** (see Supporting Information). Firstly, tetraethylene glycol was singly functionalized with a toluene sulfonyl group, followed by reaction with sodium azide to obtain the azide-terminated oligomer in a 93% yield. The hydroxyl group was activated with 1,1-carbonyldiimidazole (CDI), and further reacted with an excess of a trityl (Trt)-protected linear 1,8-alkyldiamine resulting in a 52% yield. The azide group was reduced by catalytic hydrogenation to obtain a free amine, followed by coupling with the CDI activated carboxyl of 1,2-dithiolane group to provide an amide in 69% yield. The Trt protecting group was subsequently deprotected using trifluoroacetic acid (TFA) and further reacted with dibutyl squarate to provide mono-squaramide amphiphile with the 1,2-dithiolane moiety in a 69% yield. Lastly, the dithiolane-functionalized squaramide amphiphile was reacted with a tris(2-aminoethyl)amine (TREN) to obtain the tripodal dithiolane-based monomer **SQ-DT** in a 49% yield. The one arm RGD-peptide functionalized squaramide-based monomer (**SQ-RGD**) was obtained using copper(I)-catalyzed cycloaddition (CuAAc) to couple the azide-functionalized squaramide-based monomer **SQ-A** (see **Scheme S3.2**) and an alkyne-terminated RGD peptide (see **Scheme S3.3**).

3.3.2 Preparation of supramolecular materials

We earlier demonstrated that the monomer **SQ** can form transparent hydrogels through sonication and has a critical gelation concentration (CGC) in the range of 4.0-4.60 mM in phosphate buffered saline (PBS).[43] Conversely, the monomer **SQ-**

DT containing the 1,2-dithiolane group is insoluble in deionized water or PBS (pH 7.4), even at low concentrations (0.1 mM). A co-assembly strategy was used to prepare the multicomponent hydrogels containing monomers **SQ** and **SQ-DT** (see Supporting Information). To obtain the required concentration and volume of final multicomponent hydrogels **SQ/xSQ-DT** (x: molar perecent of **SQ-DT**), DMSO stock solutions of **SQ** (10 mM) and **SQ-DT** (5 mM) were first mixed in the appropriate ratio, followed by removing the DMSO solvent using a stream of nitrogen or air overnight to achieve a dried film of the mixture. Co-sonication of pre-made **SQ/10SQ-DT** mixed monomers in an ice bath (~ 0 °C) resulted in the formation of a clear solution that was then incubated at 37 °C in oven for 15 min or at room temperature overnight providing transparent hydrogels with reduced CGC value (0.4-1.0 mM) (see **Figure S3.1**, Supporting Information). Further increasing the molar percentage of **SQ-DT** to 20 mol% reduced the solubility during the co-sonication process and caused slight turbid solution formation after sonication. Hereafter, we focus on the mixture containing **SQ/10SQ-DT** that has 10 mol% of **SQ-DT** and 90 mol% of the native monomer **SQ** to understand their co-assembly and applications in 3D cell culture. The same procedure as mentioned above was used to prepare the multicomponent hydrogels **SQ/10SQ-DT/ySQ-RGD** (y: molar percent of **SQ-RGD**).

3.3.3 Modulation of the mechanical properties of supramolecular materials using UV light irradiation

The mechanical properties of two-component supramolecular hydrogels in PBS (pH 7.4) without or with light exposure were collected by oscillatory rheology at room temperature. The soft supramolecular hydrogels (**SQ/10SQ-DT**) were prepared through sonication and being left to stand overnight, resulting in a wide range of storage moduli (G'), ranging from 5.9 ± 0.4 Pa to 440 ± 34 Pa on increasing the total monomer concentration from 1.0 mM to 12.0 mM before the application of UV light (**Figure S3.2**). The hydrogels were then further stiffened with the application of UV light (~10 mW/cm^2, a broad wavelength from 320 to 500 nm, with a primary peak at 365 nm) consistent with the formation of crosslinks between the 1,2-dithiolane moieties. The stiffening of the hydrogel could be achieved efficiently in less than 10 minutes and without the use of a photoinitiator, for example, a G' of 17490 ± 1748 Pa was achieved when a total monomer concentration of 12.0 mM containing 1.2 mM **SQ-DT** was used (**Figure 3.2A, B**).

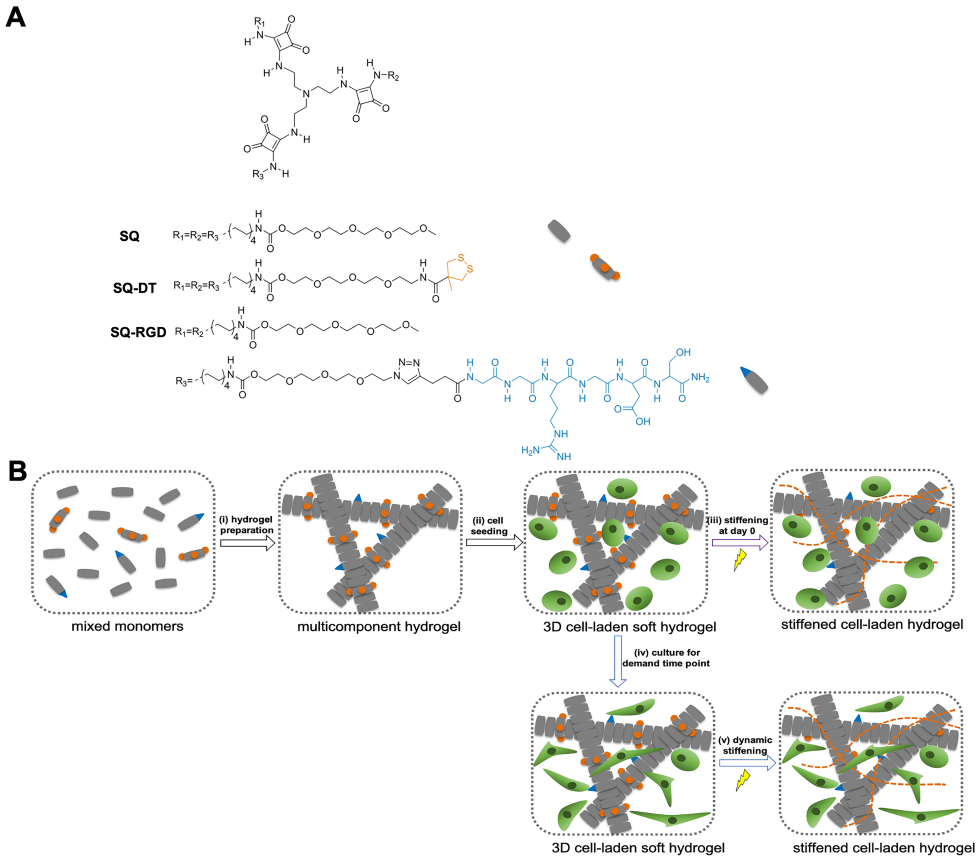

Figure 3.1 (A) Chemical structures of tripodal squaramide-based monomers **SQ**, **SQ-DT** and **SQ-RGD**. (B) Multicomponent supramolecular materials (**SQ/xSQ-DT/ySQ-RGD**) preparation and protocol for 3D cell culture experiments involving dynamic stiffening using UV light: (i) sonication of monomer mixtures in PBS (pH 7.4) in an ice bath to obtain a clear solution; followed by 15 min equilibration at 37 °C to trigger hydrogel formation before being left to stand overnight; (ii) Mixing of a single cell suspension with the pre-made hydrogels by gently pipetting up and down several times; (iii) Cell-laden supramolecular hydrogels could be directly exposed to UV light for 5 min on day 0 or (iv) left as is after seeding without exposure to UV light; (v) Dynamic stiffening of the cell-laden supramolecular hydrogels after 24 h or 48 h culture. UV irradiation was applied using a benchtop LED source (~10.0 mW/cm^2, 375 nm).

The potential to modulate the mechanical properties of hydrogels (**SQ/10SQ-DT**) using UV light (e.g., light intensity, light irradiation time) was further examined. The time to reach a plateau in the storage modulus G' was reduced from ~8 min to ~6 min when the light intensity was increased from ~5.0 mW/cm^2 to ~20.0 mW/cm^2. However, they reached comparable G' values at a plateau when given enough time (e.g., 10 min) for photocrosslinking to occur for all light intensities examined (**Figure S3.4**). The time of light exposure was also

found to affect the final G' value. For example, a higher final G' was achieved when longer UV irradiation times are applied to the material to consume all photo-reactive groups (**Figure S3.5**). Importantly, the G' of the supramolecular hydrogel could be controlled in a step-wise fashion opening the door for applications that require spatial or temporal control over hydrogel properties (**Figure 3.2C**).

To explore their self-recovery properties before and after UV irradiation with the added disulfide crosslinks (through radical reorganization or ring opening polymerization) in the supramolecular polymer network, a step-strain experiment was performed. A high strain (500%) was first applied to the hydrogel outside of its linear viscoelastic range, followed by the application of a low strain (0.05%) for 120 s, and then the cycle was repeated. The recovery of G' of all the hydrogels tested before UV light irradiation was found to be between 80%-100% of their original state, due to the reversible nature of the non-covalent interactions from the self-assembled supramolecular monomers (**Figure S3.6**). After 10 min UV light irradiation, the hydrogels still showed some self-recovery although to a lesser extent when compared to prior UV light irradiation (**Figure S3.6**). Taking the 8.0 mM **SQ/10SQ-DT** as an example, the G' of hydrogel without UV light irradiation recovered ~93% of its initial G' value, while the G' of the same hydrogel after 10 min of UV irradiation retuned ~60% of the total (**Figure 3.2D**). Compared with other 1,2-dithiolane-based adaptable hydrogel materials,[32,36] a reduction in the recovery rate after the application of high strain was observed. Ellman's test was further conducted to further examine the contribution of the thiol-disulfide exchange reaction on the observed self-recovery properties. As shown in **Figures S3.12-S3.14**, the absorbance at 412 nm caused by the free thiol production (~ 0.44 μM) in both supramolecular solutions and hydrogels with UV irradiation (5 min and 10 min) was slightly increased, indicating the limited hydrogen (α-C−H) could be abstracted by the thiyl radical in our monomer structures during the UV irradiation process.[36] This may describe their decreased self-recovery ability in our UV light irradiated hydrogels.

To further evaluate their stability for 3D cell culture applications, the viscoelastic properties of the supramolecular hydrogels (4.0 mM **SQ/10SQ-DT**) were characterized after swelling in PBS (pH 7.4) or cell culture medium DMEM (containing 20% serum) in an incubator at 37°C. When given the same UV exposure (~10 mW/cm^2, 10 min), the G' at the plateau before and after swelling in PBS/DMEM are comparable for different time points, e.g., day 1, 3 and 7 (**Figure**

S3.7). This result indicates that the **SQ-DT** containing hydrogels remain stable prior to UV light irradiation and the hydrogel can be stiffened at user-defined time points.

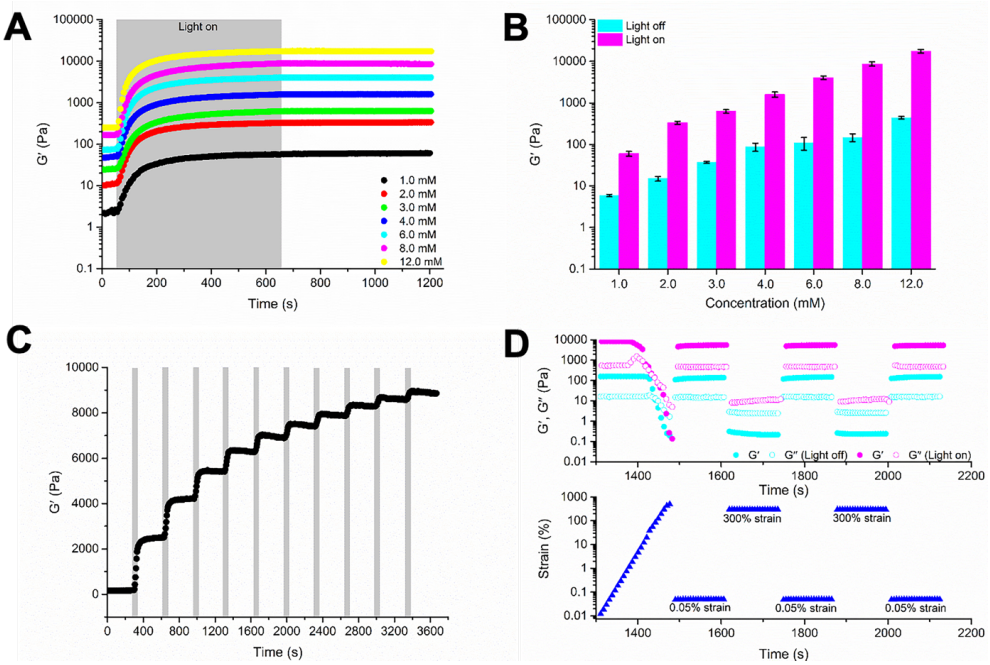

Figure 3.2 (A) Averaged (N≥3) time sweep measurements of hydrogel system (**SQ/10SQ-DT**) with varied monomer concentrations using 10 min UV light irradiation using a fixed strain (γ = 0.05%) and frequency (f = 1.0 Hz) at room temperature. (B) Plateau storage moduli (G') of **SQ/10SQ-DT** (1.0-12.0 mM) hydrogels without and with 10 min UV light irradiation. (C) The time sweep measurements of **SQ/10SQ-DT** (8.0 mM) hydrogels with UV light applied in a stepwise manner at room temperature. (D) Averaged (N≥3) strain sweep and step-strain experiments of **SQ/10SQ-DT** (8.0 mM) without and with 10 min UV light irradiation. Conditions for UV light irradiation: ~10 mW/cm^2, 320-500 nm filter with maximum absorbance at 365 nm. The shaded area indicates when the light source was applied. Error bars were calculated according the average of repeat measurements (N≥3).

3.3.4 Structural characterization of supramolecular materials before and after UV light irradiation

Cryogenic transmission electron (cryo-TEM) microscopy was performed to image the nanostructural features of the formed networks. As shown in **Figure 3.3A, B**, the imaged supramolecular hydrogels (2.0 mM **SQ/10SQ-DT**) without and with 10 min UV light irradiation both presented entangled fibers on the micron scale. When UV irradiation was applied to the gel, an increase in the fiber density was observed consistent with the measured rheological properties of the material.

However, there was no remarkable change in the fiber width under different conditions, with fibre widths of 4.5 ± 0.9 nm and 3.8 ± 0.8 nm for hydrogel without and with 10 min UV light irradiation, respectively (insert figures in **Figure 3.3A, B**). Small-angle X-ray scattering experiments (SAXS) on the supramolecular materials (**SQ/10SQ-DT**) were further performed. As shown in **Figure 3.3C, D**, in the whole q-range for the tested two different concentrations (e.g., 0.8 mM and 2.0 mM), there was an overlap of the scatting profiles for the hydrogels before and after UV irradiation, demonstrating insignificant changes in the nanoscale structures of the **SQ-DT** fibers on UV induced crosslinking. Moreover, the slope from the low q-range for all the measured samples proved their high-aspect-ratio 1D aggregates, which was consistent with the cryo-TEM results. Furthermore, a form factor of flexible cylinders was best fitting the scattering data with a fiber radius of 2.5 nm and a Kuhn length of 7.4 nm for hydrogel (2.0 mM) without UV irradiation and a fiber radius of 2.4 nm and a Kuhn length of 11.8 nm for hydrogel (2.0 mM) with 5 min UV irradiation (**Figure S3.15**).

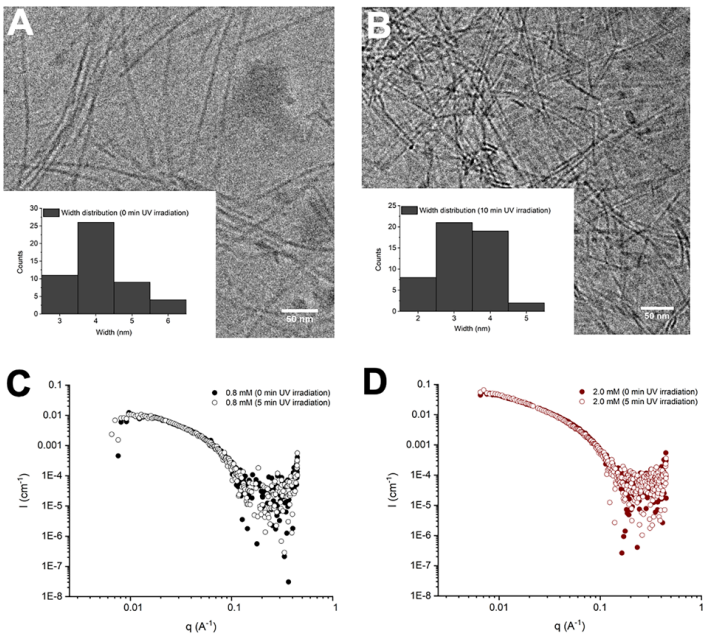

Figure 3.3 Cryo-EM images of multicomponent materials **SQ/10SQ-DT** (2.0 mM) with (A) 0 min and (B) 10 min UV irradiation using a benchtop LED source (~10 mW/cm^2, 375 nm). Scale bar: *50 nm*. The insert figures indicate the histograms of the width distribution of the counted fibers (N = 50) counted from the cryo-EM images. Small-angle X-ray scatting profiles of different concentrations of supramolecular hydrogels **SQ/10SQ-DT** before and after UV irradiation for 5 min: (C) 0.8 mM and (D) 2.0 mM.

3.3.5 Spatial and temporal patterning of bioactive cues in supramolecular materials containing 1,2-dithiolanes using UV light irradiation

We further explored the possibility of using a new chemical strategy for spatiotemporal photopatterning of biochemical cues in supramolecular materials using a dithiolane-modified cell-adhesive peptide (e.g., RGD) within the supramolecular hydrogel (**SQ/10SQ-DT**). An RGD peptide, (**(fluorescein)GK(DT)GGGRGDS**)[37] was functionalized with both fluorescein dye and DT to visualize the coupled RGD peptide in the hydrogel through UV light irradiation using either a photomask or direct laser writing (DLW) (**Figure 3.4A**). The RGD-peptide was spatially patterned through the volume of hydrogel using the UV-induced crosslinking of dithiolane by illumination through a photomask with a benchtop LED (5 min, ~10 mW/cm^2, 375 nm). The concentration of bound RGD varies on going from patterned to unppatterned areas (**Figure 3.4B**). Moreover, using two-photon lasers, fully 3D patterned volumes can be directly laser-written into the hydrogel at cell-sized relevant length scales. This further highlights the potential for spatial and/or temporal control of the network properties by introducing RGD peptides and changes to the physical properties of the network in a user-defined manner through the 1,2-dithiolane moiety, even after its initial cell seeding.

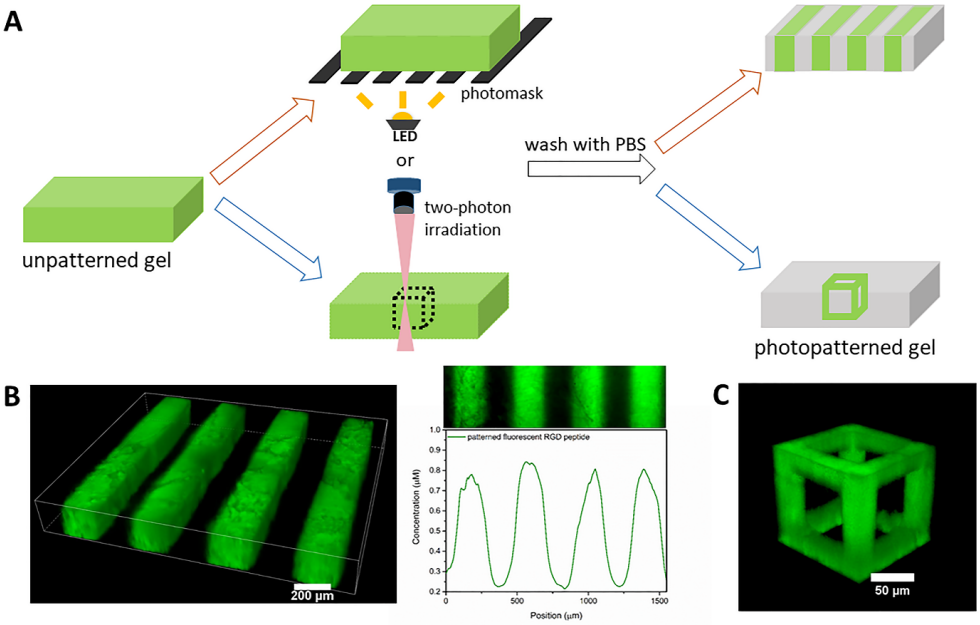

Figure 3.4 (A) Spatial and temporal patterning of a fluorescent RGD peptide (**(fluorescein)GK(DT)GGGRGDS**) within the supramolecular materials **SQ/10SQ-DT** (6.0 mM) using a photomask or two-photon laser lithography technology. (B) 3D confocal fluorescence images of fluorescent RGD peptide patterned within hydrogel under photomask for 5 min UV irradiation through a benchtop LED source (~10.0 mW/cm^2, 375 nm) and the presented patterned RGD concentration (patterned and unpatterned area). Scale bar: *200 µm*. (C) Confocal microcoscopy images of a fluorescent cube-like structure prepared by two-photon direct laser writing (DLW) using a fluorescent RGD peptide. Scale bar: *50 µm*.

3.3.6 Cells remain viable in supramolecular materials with UV light irradiation

We earlier demonstrated that squaramide-based hydrogels are cytocompatible response for several cell types, including cells that are sensitive such as induced pluripotent stem cells, in our previous work.[43] We further examined the effect of incorporating the 1,2-dithiolane unit into supramolecular materials and UV light irradiation on cells cultured within the supramolecular materials. Three different cell lines (NIH 3T3, Hs578T, and C2C12) were selected and evaluated within the materials with respect to cytocompatibility. Cell suspensions were readily mixed with the hydrogel using its self-recovery property by gentle pippeting up and down several times (**Figure 3.1B**). As shown in **Figure 3.5A**, after pipetting, all cells were homogenously dispersed throughout the hydrogel material (in 3D) after 24 h of seeding, and LIVE/DEAD assays on conditions before and after UV light irradiation (5 min) were performed. After 24 h post-encapsulation, 92 ± 4% of NIH 3T3 cells, 93 ± 1% of Hs578T cells and 89 ± 3% of C2C12 cells remained viable

without UV light irradiation (**Figure 3.5B**). When the 3D cell-laden hydrogels were stiffened further, using 5 min UV irradiation, the percentage of cell viability was slightly decreased, between 85 ± 4%-90 ± 2% for all cell lines tested. The cell viability provides an indication of the cytocompatibility of the supramolecular materials for 3D cell culture applications involving light. However, further examining the effect of UV exposure and radical formation during chemical crosslinking of 1,2-dithiolane on cell metabolism and their genomes is necessary.

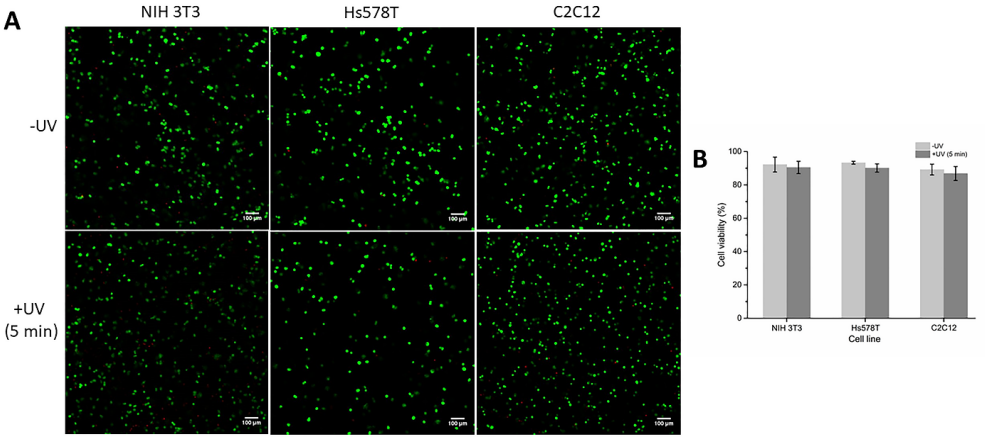

Figure 3.5 (A) Confocal microscopy images of three cells lines (NIH 3T3, Hs578T, and C2C12) stained by calcein AM and PI and (B) quantification of averaged (N = 3) cell viability of the tested cell lines after 24 h encapsulation within hydrogel **SQ/10SQ-DT** (4.0 mM) without and with 5 min UV irradiation using a benchtop LED source (~10 mW/cm^2, 375 nm). Scale bar: *100 μm*. Viable cells are labeled in green and dead cells in red. The independent repeat measurements (N = 3) were performed to obtain the error bars.

3.3.7 Photopatterned cell-adhesive peptides in supramolecular materials modulate the cell morphology

To further assess how RGD peptide-patterned supramolecular materials can spatially guide cell behavior, the morphology of C2C12 cells was quantified after encapsulation in both uniform and photopatterned hydrogels. As shown in **Figure 3.6A-D**, most of the C2C12 cells are spread after a 3-day culture period in the **SQ/10SQ-DT** (3.0 mM) hydrogel containing **DT-RGD** peptide (0.4 mM) (**Figure 3.6A**). When the hydrogel is stiffened directly after cell encapsulation, cell spreading is impeded (**Figure 3.6B**). The cells are round when encapsulated in hydrogels containing the same concentration of non-adhesive peptide **DT-DGR** instead of **DT-RGD**, in assays that are with and without UV irradiation. When

examing the capacity to spatially pattern peptides within the supramolecular material, the hydrogel (**SQ/10SQ-DT**, 3.0 mM) was mixed with a 0.4 mM RGD solution containing **DT-RGD** and **(fluorescein)GK(DT)GGGRGDS**. Then, C2C12 were encapsulated within the hydrogels followed by UV photopatterning through a photomask (with stripe 200 μm). The cells showed a more spread morphology in the fluorescent, and thus photopatterned regions where the RGD was coupled to the material (**Figure 3.6E**). Cell circularity was further quantified for C2C12 cells (**Figure 3.6F**) in both the RGD patterned areas (*green*) and non-RGD patterned areas (*black*), showing the decreasing of circularity value from 0.906 ± 0.023 to 0.805 ± 0.019 and the increasing of the elongation owing to the coupled RGD peptide. The possibility to bind RGD on-demand throughout the supramolecular hydrogels (**SQ/10SQ-DT**) with **DT-RGD** and the application of UV light to enable crosslinking of the peptide cue, is a generic strategy to introduce bioactive cues into supramolecular materials.

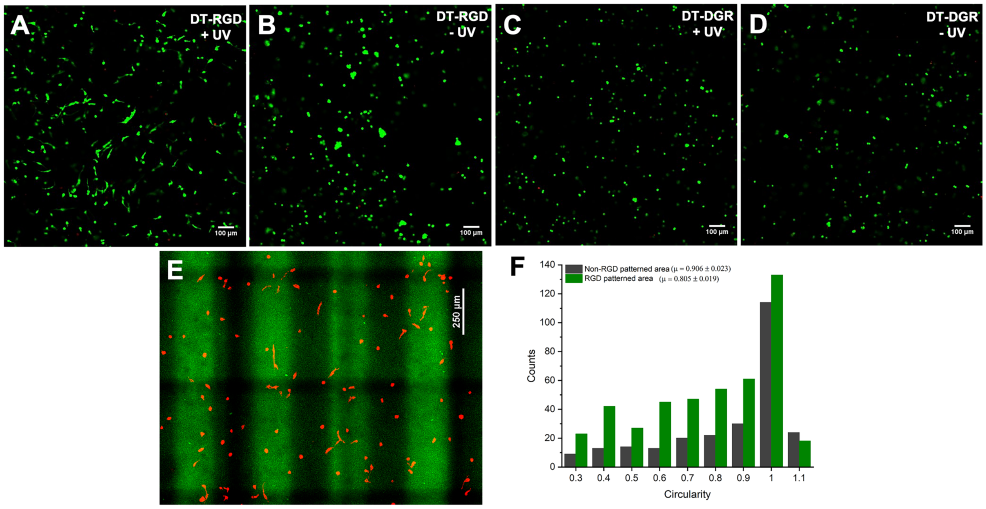

Figure 3.6 Confocal images of C2C12 cells after 3 days encapsulating in the hydrogel **SQ/10SQ-DT** (3.0 mM) with/without uniform and photopatterning RGD or DRG peptides: containing **DT-RGD** (0.4 mM) (A) with 5 min UV irradiation and (B) without UV irradiation; containing **DT-DGR** (0.4 mM) (C) with 5 min UV irradiation and (D) without UV irradiation. Scale bar: *100 μm*. C2C12 cells were stained with calcein AM (viable cells, *green*) and PI (dead cells, *red*). (E) Z projection of the confoncal image of the encapsulated C2C12 after 3 days culture in photopatterned hydrogel under photomask for 5 min UV irradiation. The hydrogel **SQ/10SQ-DT** (3.0 mM) contains **DT-RGD** (0.399 mM) and fluorescent RGD peptide (**(fluorescein)GK(DT)GGGRGDS**) (0.001 mM) with the total RGD peptide concentration (0.4 mM). Scale bar: *250 μm*. Cells were stained with rhodamine phalloidin to visualize F-actin and the green area indicated the RGD patterned area. (F) The distribution of counted C2C12 cells circularity in the RGD patterned (*green*) and un-patterned area (*black*) from image **E**. UV irradiation was applied through a benchtop LED (~10 mW/cm^2, 375 nm).

3.3.8 C2C12 myoblasts encapsulated in dynamically stiffened supramolecular materials respond with changes in cell shape

Mechanotransduction is a process where the cell responds to the mechanics of its environment with a biochemical output ultimately affecting numerous cell functions.[44,45] The transcriptional coactivator Yes-associated protein-1 (YAP) plays an important role in this mechanosensitive procedure, as the cells can sense and react by modifying the location of this protein in the cell.[44] For example, in 3D soft materials, the phosphorylation of YAP occurs in the cytoplasm and cells respond show a spread morphology.[46] Thus, integrin binding, network degradation and hydrogel stiffness are important factors to affect cellular response and morphology in 3D matrices.[47] We therefore sought to determine if a similar response of encapsulated cells to a dynamic change in stiffness occurs in our supramolecular hydrogels.

Although the RGD peptide can be introduced into the hydrogel network by photochemical crosslinking with UV light, hydrogel stiffness due to the dithiolane group on the network is also increased (see rheology data from **Figure S3.8**). Therefore, to decouple the effect of the RGD peptide and hydrogel stiffness on cell behavior, an **SQ-RGD** monomer was designed and synthesized. The three-component based supramolecular hydrogels (**SQ/10SQ-DTR/ySQ-RGD**) were prepared using the same co-assembly method above. In this way, the influence of the RGD peptide and hydrogel stiffness on cell behavior can by decoupled and be controlled on-demand by varying the added amount of **SQ-RGD** and **SQ-DT** or by modulation of the light source.

First, the multicomponent hydrogel **SQ/10SQ-DT** (6.0 mM), containing different concentrations of **SQ-RGD** (e.g., 0 mM, 0.1 mM, 0.2 mM and 0.4 mM) was prepared, and their effect on the morphology of mCherry-LifeAct C2C12 cells prior to UV irradiation was studied. After 24 h culture in 3D, cells started spreading at 0.1 mM **SQ-RGD**, and spread more at higher concentrations of 0.2 mM and 0.4 mM **SQ-RGD** from the confocal images (**Figure S3.19**). When the stiffness of the supramolecular hydrogels was further modulated by UV irradiation, cell morphology was evaluated. After 24 h culture in **SQ/10SQ-DT/3.4SQ-RGD** (6.0 mM total concentration consist of 0.2 mM **SQ-RGD**), mCherry-LifeAct C2C12 cells were well spread in the hydrogel without light irradiation (G': 85 ± 7 Pa). While most of the cells retained a round morphology when the gel was stiffened (by 5 min irradiation, G': 1476 ± 196 Pa) directly after encapsulation (**Figure 3.7A, B**). The difference in spreading was further quantified by calculating cell circularity for cells encapsulated in various hydrogels, as expected, the circulation for cells in the stiffened hydrogel increased to 0.69 ± 0.054 from 0.41 ± 0.043 in soft hydrogel without UV irradiation (**Figure 3.7C**). Conversely, when cells were allowed to spread (**Figure 3.7D**) and the gel was only stiffened after 24 hrs of culture, C2C12 retained its spread state beyond day 3 of culture (**Figure 3.7E**). There was also no significant change from the quantified cell circulation values, e.g., circulation of 0.436 ± 0.041 for cells in soft hydrogel and circulation of 0.365 ± 0.034 for cells in hydrogel dynamic stiffened with 5 min UV irradiation at 24 h (**Figure 3.7F**). Moreover, the calculated value of the larger skeleton branch length and lower aspect ratio was consistent with the trend of the smaller cell circulation, which further indicated the different hydrogel stiffness and also the stiffening time point influence the cell spread and branched morphology.

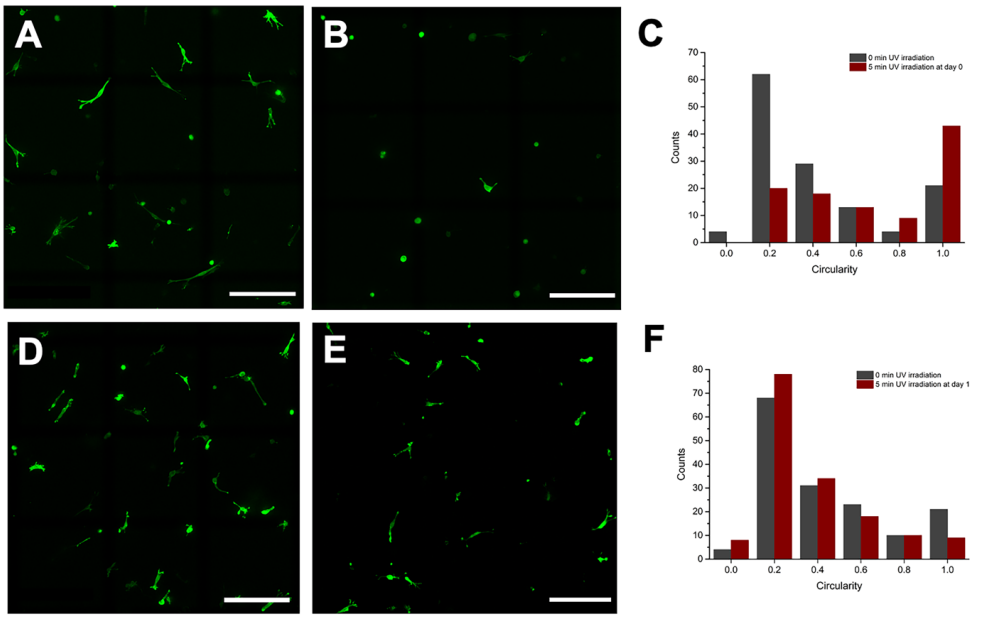

Figure 3.7 mCherry-LifeAct C2C12 myoblasts were encapsulated in **SQ/10SQ-DT/3.4SQ-RGD** hydrogels (6.0 mM) with varied stiffness by applying UV irradiation at user-demand time points. Representative confocal images of C2C12 cells after 24 h culture in hydrogel (A) without UV irradiation (G': 85 ± 7 Pa), (B) 5 min UV irradiation (G': 1476 ± 196 Pa) after seeding at day 0 and (C) corresponding distribution of the cell circularity. Confocal images of C2C12 cells after 3 days culture in hydrogels (D) without UV irradiation, (E) 5 min UV irradiation at day 1 and (F) corresponding distribution of the cell circularity within the measured systems. The UV irradiation was applied using a benchtop LED (~10 mW/cm^2, 375 nm).

3.3.9 Hs578T breast cancer cells encapsulated in dynamically stiffened supramolecular materials respond with changes in cell shape and migration

Metastasis is the leading cause of death for cancer patients. Hydrogel scaffolds have been explored to mimic the tumor microenvironment *in vitro* to understand this invasion process *in vivo*. For example, breast cancer cells exhibited decreased invasion in stiffer covalent hydrogels, with matrix metalloproteinase crosslinks necessary for migration to take place through degradation.[21,48-50] However, cell-mediated degradation of the covalent hydrogels would change the local stiffness of gel and eventual gel degradation during longer culture times.[51] Here, we examined the use of our fibrillar, self-assembled supramolecular hydrogels that self-recover to aid in cancer cell migration because of the physical nature of the interactions that hold them together. More importantly, the dynamic change in

stiffness of the hydrogel would provide a new angle to further understand this complex process.

The migration of mCherry-LifeAct Hs578T breast cancer cells within the hydrogel **SQ/10SQ-DT/10SQ-RGD** (4.0 mM) was further examined. As shown in the representative confocal image in **Figure S3.20**, cells showed a spread morphology in the soft, supramolecular hydrogel material (G'~ 40 Pa) before UV irradiation. However, the cells remained round when the hydrogels were directly stiffened after seeding. The reduction of cell circularities, from 1.016 ± 0.038 for 5 min UV irradiation to 0.799 ± 0.03 for 0 min UV irradiation, further illustrates the confining effect of the stiffened hydrogels and the influence on cell morphology. Moreover, the dynamic change of the hydrogel stiffness on cell migration was also studied. mCherry-LifeAct Hs578T cells were first allowed to spread after 24 h culture in the soft supramolecular hydrogel material, and as expected, the spread cells migrated within the hydrogel before UV irradiation can be clearly seen through time-lapse microscopy (24-48 h). However, when the same cell-laden hydrogel was stiffened after 48 hrs of culture and imaging, the cells maintained their spread morphology. Their migratory behavior was impeded, as shown by imaging the same cells at the same position again (in the time-lapse microscopy within 48-72 h). The migration of the cells was tracked inside the hydrogels before (24-48 h) and after UV-stiffening (48-72 h) (**Figure 3.8**). The cells were found to migrate readily through the hydrogel before UV irradiation, but could only back-track their motion after the dynamic stiffening (**Figure 3.8A, B**). Both the speed and persistence migration sharply decreased, when hydrogel stiffness was increased (**Figure 8C, D**).

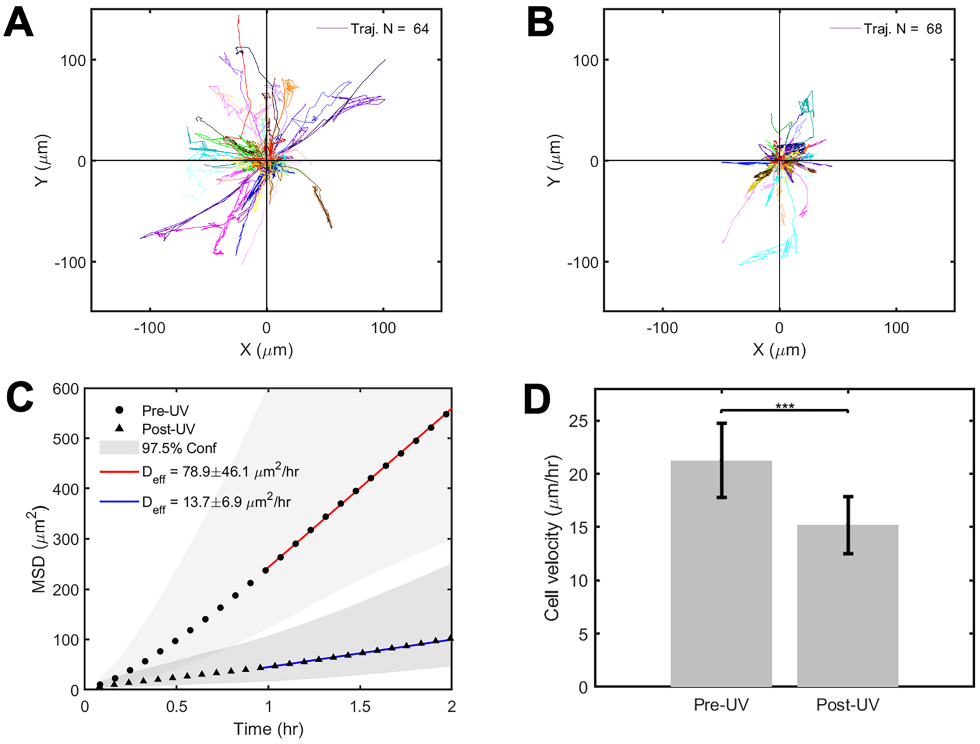

Figure 3.8 Representations of mCherry-LifeAct Hs578T cells trajectories within hydrogel **SQ/10SQ-DT/10SQ-RGD** (4.0 mM): (A) cells traced for 24-48 h within hydrogel pre-UV irradiation; (B) cells traced for 48-72 h after post-UV irradiation (5 min) after 48 h using a benchtop LED (~10.0 mW/cm^2, 375 nm). (C) Mean-squared displacement (MSD) of the tracked trajectories within hydrogels with varied stiffness pre- and post-UV irradiation. (D) The effect of the hydrogel stiffness on cell velocity.

3.4 Conclusions

A novel tripodal squaramide-based supramolecular monomer was end-functionalized with light-activatable 1,2-dithiolane (DT) moieties and examined for its capacity to prepare spatiotemporally responsive hydrogel materials. The multicomponent supramolecular materials were obtained through co-assembly of the dithiolane-based monomer with a native squaramide monomer. Their mechanical stiffness could be increased to 10 kPa under UV irradiation without affecting fiber morphology and nanoscale structures of the network. The wide stiffness range can be tuned by varying the monomer concentration or the parameters of the light source. The hydrogels after UV exposure showed some self-recovery properties due to the combination of the non-covalent crosslinks and disulfide based covalent crosslinks. Moreover, the mechanical properties can also be temporally controlled in a step-wise manner and the bioactive cues such as the RGD peptide can be introduced spatially by photopatterning under photomask or direct laser writing. 3D cell culture of three cell lines (NIH 3T3, C2C12, Hs578T) within the supramolecular materials showed a cytocompatible response in response to photo-induced dithiolane based chemical reactions within the tested conditions. The RGD-functionalized squaramide based monomer can be further incorporated into the supramolecular hydrogels through the co-assembly strategy for decoupling of hydrogel stiffness and bioactive cues on cell behavior and providing the integrin site for the cells to bind. Unlike traditional covalent networks without degradation sites, our hierarchically self-assembled supramolecular materials with reversible physical crosslinks could be pushed and remodeled by the cells after sensing the varied mechanical stiffness, which resulted in the change of the cell morphology and migration. Morphology of C2C12 cells encapsulated in supramolecular materials can be modulated by varying hydrogel stiffness or delaying the onset of stiffening the material. Finally, change in the dynamics of Hs578T breast cancer cell migration was achieved through stiffening the hydrogel materials at specific time points. The simple and cytocompatible strategy to spatially and temporally the hierarchical properties of supramolecular materials using UV light broadens the application of self-assembled supramolecular hydrogels to create more complex and dynamic artificial matrix platforms *in vitro* cell culture.

3.5 References

(1) Daley, W. P.; Peters, S. B.; Larsen, M. *J. Cell Sci.* **2008**, *121* (3), 255-264.

(2) Lu, P.; Takai, K.; Weaver, V. M.; Werb, Z. *Cold Spring Harb. Perspect. Biol.* **2011**, *3* (12), a005058.

(3) Gattazzo, F.; Urciuolo, A.; Bonaldo, P. *Biochim. Biophys. Acta* **2014**, *1840* (8), 2506-2519.

(4) Uto, K.; Tsui, J. H.; DeForest, C. A.; Kim, D. H. *Prog. Polym. Sci.* **2017**, *65*, 53-82.

(5) Walker, C.; Mojares, E.; Del Rio Hernandez, A. *Int. J. Mol. Sci.* **2018**, *19* (10), 3028.

(6) Meli, V. S.; Veerasubramanian, P. K.; Atcha, H.; Reitz, Z.; Downing, T. L.; Liu, W. F. *J. Leukoc. Biol.* **2019**, *106* (2), 283-299.

(7) Huang, G.; Li, F.; Zhao, X.; Ma, Y.; Li, Y.; Lin, M.; Jin, G.; Lu, T. J.; Genin, G. M.; Xu, F. *Chem. Rev.* **2017**, *117* (20), 12764-12850.

(8) Gillette, B. M.; Jensen, J. A.; Wang, M.; Tchao, J.; Sia, S. K. *Adv. Mater.* **2010**, *22* (6), 686-691.

(9) Kloxin, A. M.; Tibbitt, M. W.; Kasko, A. M.; Fairbairn, J. A.; Anseth, K. S. *Adv. Mater.* **2010**, *22* (1), 61-66.

(10) Manaster, B. J. *Diagn. Radiol.* **2009**, *2009*, 70-72.

(11) Khetan, S.; Burdick, J. A. *Biomaterials* **2010**, *31* (32), 8228-8234.

(12) DeForest, C. A.; Anseth, K. S. *Nat. Chem.* **2011**, *3* (12), 925-931.

(13) Khetan, S.; Guvendiren, M.; Legant, W. R.; Cohen, D. M.; Chen, C. S.; Burdick, J. A. *Nat. Mater.* **2013**, *12* (5), 458-465.

(14) Stowers, R. S.; Allen, S. C.; Suggs, L. J. *Proc. Natl. Acad. Sci. U. S. A.* **2015**, *112* (7), 1953-1958.

(15) Mosiewicz, K. A.; Kolb, L.; van der Vlies, A. J.; Lutolf, M. P. *Biomater. Sci.* **2014**, *2* (11), 1640-1651.

(16) Brown, T. E.; Silver, J. S.; Worrell, B. T.; Marozas, I. A.; Yavitt, F. M.; Gunay, K. A.; Bowman, C. N.; Anseth, K. S. *J. Am. Chem. Soc.* **2018**, *140* (37), 11585-11588.

(17) Yavitt, F. M.; Brown, T. E.; Hushka, E. A.; Brown, M. E.; Gjorevski, N.; Dempsey, P. J.; Lutolf, M. P.; Anseth, K. S. *Adv. Mater.* **2020**, *32* (30), e1905366.

(18) Burdick, J. A.; Murphy, W. L. *Nat. Commun.* **2012**, *3* (1), 1-8.

(19) Brown, T. E.; Anseth, K. S. *Chem. Soc. Rev.* **2017**, *46* (21), 6532-6552.

(20) LeValley, P. J.; Kloxin, A. M. *ACS Macro Lett.* **2019**, *8* (1), 7-16.

(21) Rosales, A. M.; Anseth, K. S. *Nat. Rev. Mater.* **2016**, *1* (2), 1-15.

(22) Song, S.; Wang, J.; Cheng, Z.; Yang, Z.; Shi, L.; Yu, Z. *Chem. Sci.* **2020**, *11* (5), 1383-1393.

(23) He, M.; Li, J.; Tan, S.; Wang, R.; Zhang, Y. *J. Am. Chem. Soc.* **2013**, *135* (50), 18718-18721.

(24) Boekhoven, J.; Stupp, S. I. *Adv. Mater.* **2014**, *26* (11), 1642-1659.

(25) Dong, R.; Pang, Y.; Su, Y.; Zhu, X. *Biomater. Sci.* **2015**, *3* (7), 937-954.

(26) Webber, M. J.; Appel, E. A.; Meijer, E. W.; Langer, R. *Nat. Mater.* **2016**, *15* (1), 13-26.

(27) Zhou, J.; Li, J.; Du, X.; Xu, B. *Biomaterials* **2017**, *129*, 1-27.

(28) Dou, X. Q.; Feng, C. L. *Adv. Mater.* **2017**, *29* (16), 1604062.
(29) Arkenberg, M. R.; Nguyen, H. D.; Lin, C. C. *J. Mater. Chem. B* **2020**, *8* (35), 7835-7855.
(30) Wang, H.; Heilshorn, S. C. *Adv. Mater.* **2015**, *27* (25), 3717-3736.
(31) Goethals, F.; Frank, D.; Du Prez, F. *Prog. Polym. Sci.* **2017**, *64*, 76-113.
(32) Barcan, G. A.; Zhang, X.; Waymouth, R. M. *J. Am. Chem. Soc.* **2015**, *137* (17), 5650-5653.
(33) Zhang, X.; Waymouth, R. M. *J. Am. Chem. Soc.* **2017**, *139* (10), 3822-3833.
(34) Yu, H.; Wang, Y.; Yang, H.; Peng, K.; Zhang, X. *J. Mater. Chem. B* **2017**, *5* (22), 4121-4127.
(35) Song, L.; Zhang, B.; Gao, G.; Xiao, C.; Li, G. *Eur. Polym. J.* **2019**, *115*, 346-355.
(36) Scheutz, G. M.; Rowell, J. L.; Ellison, S. T.; Garrison, J. B.; Angelini, T. E.; Sumerlin, B. S. *Macromolecules* **2020**, *53* (10), 4038-4046.
(37) Tong, C.; Wondergem, J. A. J.; Heinrich, D.; Kieltyka, R. E. *ACS Macro Lett.* **2020**, *9* (6), 882-888.
(38) Storer, R. I.; Aciro, C.; Jones, L. H. *Chem. Soc. Rev.* **2011**, *40* (5), 2330-2346.
(39) Wurm, F. R.; Klok, H. A. *Chem. Soc. Rev.* **2013**, *42* (21), 8220-8236.
(40) Marchetti, L. A.; Kumawat, L. K.; Mao, N.; Stephens, J. C.; Elmes, R. B. P. *Chem* **2019**, *5* (6), 1398-1485.
(41) Saez Talens, V.; Englebienne, P.; Trinh, T. T.; Noteborn, W. E.; Voets, I. K.; Kieltyka, R. E. *Angew. Chem. Int. Ed.* **2015**, *54* (36), 10502-10506.
(42) Saez Talens, V.; Makurat, D. M. M.; Liu, T.; Dai, W.; Guibert, C.; Noteborn, W. E. M.; Voets, I. K.; Kieltyka, R. E. *Polym. Chem.* **2019**, *10* (23), 3146-3153.
(43) Tong, C.; Liu, T.; Saez Talens, V.; Noteborn, W. E. M.; Sharp, T. H.; Hendrix, M.; Voets, I. K.; Mummery, C. L.; Orlova, V. V.; Kieltyka, R. E. *Biomacromolecules* **2018**, *19* (4), 1091-1099.
(44) Dupont, S.; Morsut, L.; Aragona, M.; Enzo, E.; Giulitti, S.; Cordenonsi, M.; Zanconato, F.; Le Digabel, J.; Forcato, M.; Bicciato, S.; Elvassore, N.; Piccolo, S. *Nature* **2011**, *474* (7350), 179-83.
(45) Wolfenson, H.; Yang, B.; Sheetz, M. P. *Annu. Rev. Physiol.* **2019**, *81*, 585-605.
(46) Judson, R. N.; Tremblay, A. M.; Knopp, P.; White, R. B.; Urcia, R.; De Bari, C.; Zammit, P. S.; Camargo, F. D.; Wackerhage, H. *J. Cell Sci.* **2012**, *125* (24), 6009-6019.
(47) Caliari, S. R.; Vega, S. L.; Kwon, M.; Soulas, E. M.; Burdick, J. A. *Biomaterials* **2016**, *103*, 314-323.
(48) Even-Ram, S.; Yamada, K. M. *Curr. Opin. Cell Biol.* **2005**, *17* (5), 524-532.
(49) Ahearne, M. *Interface Focus* **2014**, *4* (2), 20130038.
(50) J Yamada, K. M.; Sixt, M. *Nat. Rev. Mol. Cell Biol.* **2019**, *20* (12), 738-752.
(51) Doyle, A. D.; Yamada, K. M. *Exp. Cell Res.* **2016**, *343* (1), 60-66.

3.6 Supporting Information

3.6.1 Materials and instruments

The chemicals and reagents for the synthesis of squaramide-based tripodal monomers were purchased from commercial suppliers and used without further purification. Deuterated chloroform, methanol and dimethyl sulfoxide were obtained from Euriso-top. Water was deionized prior to use. Dulbecco's phosphate buffered saline (DPBS) was purchased from Sigma Aldrich. Dulbecco's modified Eagle medium (DMEM)-high glucose (D6546) was obtained from Gibco, Life Technologies. RPMI-1640 medium was achieved from Thermo Fisher Scientific. Calcein AM and propidium iodide (PI) were achieved from Sigma Aldrich. AlexaFluor488-phalloidin antibody was obtained from Invitrogen. µ-slide 4, µ-slide 8 and µ-slide 15 well plates were achieved from ibidi. Microscopy slips (#1.5, 30 mm) were obtained from Thermo Fisher Scientific. Polydimethylsiloxane (PDMS) (Sylgard 184 Silicon Elastomer Kit, Dow Corning), silicon wafer, Fluorosilane (1H,1H,2H,2H-perfluorooctyltrichlorosilane) were purchased from VWR chemicals, Siegert Wafers and Sigma Aldrich respectively. The monomer **SQ** and fluorescent dye- and 1,2-dithiolane-labeled peptide (**(Fluorescein)GK(DT)GGGRGDS**) were synthesized as reported previously.[1,2] Purification of the monomers **SQ**, **SQ-DT**, **SQ-RGD**, **DT-RGD**, **DT-DGR** and **(Fluorescein)GK(DT)GGGRGDS** were carried out by RP-HPLC on a Vydac C18 reversed phase column connected with UV detection. ^{1}H-NMR and ^{13}C-NMR spectrums were acquired on a Bruker DMX-400 operating at room temperature. LC-MS data were collected on a Finnigan Surveyor HPLC system with Gemini C18 column (50 × 4.60 mm, UV detection range: 200-600 nm) and a Finnigan LCQ Advantage Max mass spectrometer with ESI. The solvent gradient of the mobile phase for LC-MS: CH_3CN-H_2O (10-90%) with 0.1% TFA over 13.5 min. Oscillatory rheology experiments were performed at room temperature on a Discovery Hybrid Rheometer (DHR-2, TA Instruments) using a parallel plate geometry (20 mm diameter). The UV light source connected to the rheometer was obtained on an Excelitas Omnicure S2000 system (wavelength: 320-500 nm, primary peak: 365 nm) through a light guide (5 mm diameter). The copper grids (300 mesh) with a lacey-carbon support film were obtained from Electron Microscopy Sciences. The plunge-freezing procedure was carried out using a Leica EM GP (Leica Microsystems). Cryo-TEM images of samples were acquired on a Tecnai

F12 microscope (FEI) equipped with a field emission gun operating at 120 keV using a Gatan UltraScan charge-coupled device (CCD) camera. The SAXS experiments were measured on a SAXSLAB GANESHA 300 XL SAXS system equipped with a GeniX 3D Cu ultralow divergence microfocus sealed tube source producing X-rays (wavelength $\lambda = 1.54$ Å) at a flux of 1×10^8 ph/s and a Pilatus 300 K silicon pixel detector with 487 × 619 pixels of 172 × 172 µm in size placed at two sample-to-detector distances of 713 and 1513 mm, respectively, with the q-range of $0.009 \leq q \leq 0.456$ Å^{-1}, where the q was calculated from $q = 4\pi/\lambda(\sin \theta/2)$. Silver behenate was used to calibrate the beam center and the q-range. The SAXS patterns were brought to an absolute intensity scale and were azimuthally averaged to 1D SAXS profiles through using the parameters of calibrated detector response function, known sample-to-detector distance, measured incident, and transmitted beam intensities. Software of SAXS utilities (http://www.sztucki.de/SAXSutilities/) was used to subtract the scattering contribution of the solvent and quartz cell and to obtain the scattering curves. The software of SASview (http://www.sasview.org/) was used to further analyze the obtained SAXS profiles. UV-Vis spectra were collected on a Cary 300 spectrophotometer from Agilent using a quartz cuvette (path length: 1.0 cm). The photomask for the photo-patterning was designed in AutoCad (Autodesk, CA, USA) and printed on premium emulsion film at a resolution of 200k dpi (JD Photo Data, UK). Two-photon crosslinking through direct laser writing (DLW) was performed on the Photonics Professional GT (Nanoscribe GMBH, Karlsruhe Germany). The fluorescent images of photo-patterned hydrogels were acquired on a Nikon Eclipse Ti microscope equipped with a Yokogawa confocal spinning disk unit operated at 10,000 rpm (Nikon, Tokyo, Japan) using a 10x and 20x (CFI Plan Fluor, NA 0.5) objective. The images for the cell viability studies of 3D cell-laden hydrogels were collected from a Zeiss LSM 710 confocal laser scanning microscope equipped with a Zeiss 5x objective.

3.6.2 Synthetic routes and procedures

Synthesis of monomer SQ-DT

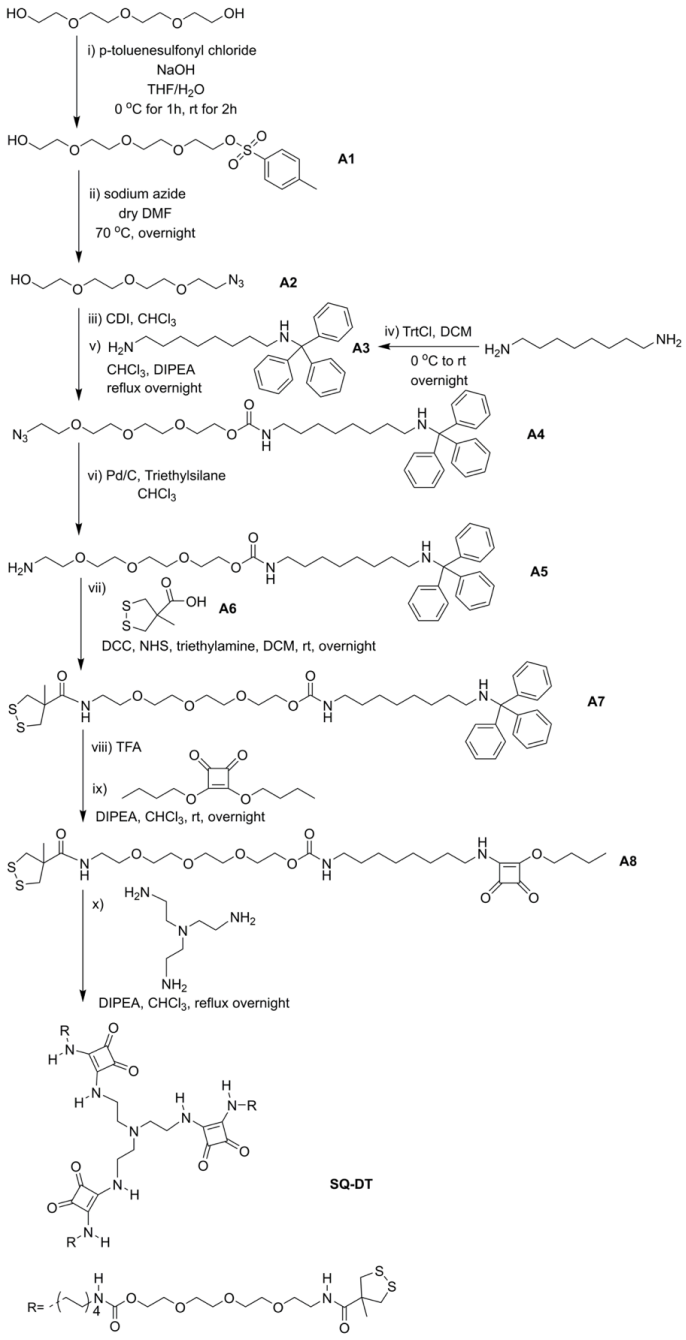

Scheme S3.1 Synthetic route of monomer **SQ-DT**.

Synthesis of compound A1

Sodium hydroxide (0.99 g, 24.75 mmol) was dissolved in water (6 mL) and was added to tetraethylene glycol (29.98 g, 154.36 mmol) in tetrahydrofuran (THF, 6 mL) in an ice bath. Then, a solution of *p*-toluene sulfonyl chloride (2.94 g, 15.44 mmol) in THF (18 mL) was added dropwise over 2 h in an ice bath to the reaction mixture. The reaction was stirred for 4 h at room temperature until the reaction was complete (as detected by TLC). Dichloromethane (DCM, 100 mL) was added and washed with water (100 mL). The aqueous fraction was extracted with DCM (3 x 100 mL) and the organic fraction was further washed with water (3 x 100 mL). The combined organic fractions were dried with Na_2SO_4, filtered, and the solvent was removed *in vacuo*. The crude product was further purified by silica column chromatography using first petroleum ether (PE)/ethyl acetate (EtOAc) (2:1, v:v) as the eluent and then EtOAc. The product was concentrated by rotary evaporation to obtain an oil-like product **A1**.

Yield: 4.52 g, 84%. ^{1}H-NMR ($CDCl_3$, 400 MHz): 7.74-7.70 (2H, m), 7.29-7.27 (2H, m), 4.10-4.06 (2H, m), 3.64-3.48 (14H, m), 2.85 (1H, s), 2.37 (3H, s). ^{13}C-NMR ($CDCl_3$, 100 MHz): 144.46, 132.43, 129.44, 127.50, 72.06, 70.22, 70.16, 70.05, 69.97, 69.83, 68.91, 68.19, 61.17, 21.20.

Synthesis of compound A2

Sodium azide (3.85 g, 59.22 mmol) was added to a stirred solution of **A1** (4.13 g, 11.85 mmol) in ethanol (34 mL). The reaction mixture was then heated to 70 °C with stirring overnight. After the reaction was complete (as detected by TLC), the white solid was filtered out and the ethanol was removed *in vacuo*. Water (100 mL) was added to the crude reaction mixture and extracted with DCM (3 x 100 mL). The combined organic fractions were dried with Na_2SO_4, filtered, and the solvent was removed *in vacuo*. The collected oil-like product **A2** was confirmed by NMR and used without further purification.

Yield: 2.44 g, 94%. ^{1}H-NMR ($CDCl_3$, 400 MHz): 3.49-3.43 (12H, m), 3.38-3.35 (2H, m), 3.27 (1H, s), 3.18-3.15 (2H, m). ^{13}C-NMR ($CDCl_3$, 100 MHz): 72.07, 70.10, 70.08, 70.05, 70.01, 69.98, 69.73, 69.47, 60.92, 50.06.

Synthesis of compound A3

1,8-Diaminooctane (16.0 g, 110.91 mmol) was first dissolved in DCM (200 mL). A solution of trityl chloride (7.73 g, 27.73 mmol) dissolved in DCM (100 mL) was then added dropwise to 1,8-Diaminooctane solution in an ice bath over 2 h, followed by stirring at room temperature overnight. Once the reaction was complete (as determined by TLC), the DCM was removed by rotary evaporation. EtOAc (100 mL) was then added and crude was washed with water (100 mL). The aqueous fraction was back-extracted with EtOAc (2 x 100 mL). The organic fractions were combined and dried with Na_2SO_4, and the solvent was removed *in vacuo*. The crude product was further purified by silica column chromatography using solvent gradient from DCM to DCM/MeOH/NH_4OH (20:1:0.1, v:v:v). The product was evaporated by rotary evaporation to obtain a yellow oil-like product **A3**.

Yield: 5.62 g, 52 %. ^{1}H-NMR ($CDCl_3$, 400 MHz): 7.51-7.49 (6H, m), 7.30-7.28 (6H, m), 7.26-7.16 (3H, m), 2.69-2.66 (2H, m), 2.14-2.11 (2H, m), 1.47-1.25 (12H, m). ^{13}C-NMR ($CDCl_3$, 100 MHz): 146.42, 128.72, 127.79, 126.19, 70.90, 43.61, 42.26, 33.77, 30.94, 29.68, 29.51, 27.38, 26.92.

Synthesis of compound A4

1,1-Carbonyldiimidazole (1.33 g, 8.20 mmol) was added to oil-like compound **A2** (1.63 g, 7.45 mmol) and stirred at room temperature without adding additional solvent. After 30 minutes, chloroform (2 mL) was added to the reaction mixture and left to stir for another 1 h at room temperature. After the reaction was completed (as determined by TLC), more chloroform (15 mL) was added to the crude, followed by the addition of compound **A3** (3.46 g, 8.95 mmol) and N, N-diisopropylethylamine (DIPEA, 1.94 mL, 11.17 mmol). The crude was refluxed overnight and completion of the reaction was determined by TLC analysis. The crude was transferred to a separatory funnel and diluted with DCM (50 mL). The organic fraction was washed with water (50 mL) and the water fraction was collected. The aqueous fraction was then back-extracted with DCM (2 x 50 mL). The combined organic fractions were dried with Na_2SO_4, filtered, and the solvent was evaporated *in vacuo*. The crude product was purified by silica column chromatography using PE/EtOAc solvent gradient (4:1 to 1:1, v:v). The product was evaporated by rotary evaporation to obtain the yellow oil-like product **A4**.

Yield: 3.57 g, 76%. ^{1}H-NMR ($CDCl_3$, 400 MHz): 7.61-7.58 (m, 6H), 7.38-7.34 (m, 6H), 7.28-7.24 (m, 3H), 5.10-5.07 (m, 1H), 4.33-4.30 (m, 2H), 3.78-3.72 (m, 12H), 3.44-3.41 (m, 2H), 3.26-3.21 (m, 2H), 2.24-2.21 (m, 2H), 1.60-1.15 (m, 12H). ^{13}C-NMR ($CDCl_3$, 100 MHz): 156.23, 146.16, 128.44, 127.54, 125.94, 70.65, 70.47, 70.44, 70.30, 69.85, 69.46, 63.57, 50.41, 43.34, 40.79, 30.64, 29.74, 29.34, 29.04, 27.07, 26.52.

Synthesis of compound A5

A4 (2.2 g, 3.48 mmol) was dissolved in dry methanol (5 mL) and dry DCM (5 mL). Palladium on carbon (39.38 mg, 0.38 mmol) was added to the clear stirring solution above. The reaction was sealed with a rubber septum and flushed with a stream of nitrogen gas over 30 minutes. Then, triethylsilane (6 mL, 37.56 mmol) was added slowly to the stirring solution over the course of 30 min. The reaction mixture was left to stir for another 3 hours at room temperature. After the reaction was complete (as determined by TLC), the mixture was filtered over celite to remove the palladium on carbon. The solvent was concentrated by rotary evaporation and further dried by a gentle stream of air. The product **A5** was directly used without further purification.

Synthesis of compound A6

Compound **A6** was synthesized according to previously published literature.[3] Briefly, 3,3′-Dichloropivalic acid (4.00 g, 23.38 mmol) was added to a 2-neck round bottom flask and water (40 mL) was added. To the stirred suspension, sodium carbonate (2.30 g, 21.71 mmol) was slowly added, followed by dropwise addition of potassium thioacetate (5.34 g, 46.78 mmol) in water (5 mL) over 10 minutes at room temperature. The resulting clear solution was heated to 100 °C and refluxed for 8 hours. Then, more sodium carbonate (7.44 g, 70.16 mmol) was added to the reaction and further refluxed at 100 °C. After the disappearance of the starting material, dimethyl sulfoxide (DMSO, 3.6 mL) was added, followed by refluxing for another 4 hours. The mixture was allowed to cool to room temperature having a basic pH (pH~9). The reaction mixture was acidified with hydrochloric acid to pH~1 resulting in the formation of a yellow precipitate. The precipitate was filtered off *in vacuo* and washed with ice-cold water 3 times. The yellow solid was left to dry *in vacuo* at room temperature overnight.

Yield: 2.93 g, 75%. ^{1}H-NMR ($CDCl_3$, 400 MHz): 3.71-3.68 (2H, d), 2.97-2.94 (2H, d), 1.54 (3H, s). ^{13}C-NMR ($CDCl_3$, 100 MHz): 181.37, 57.52, 47.72, 24.12.

Synthesis of compound A7

A6 (0.68 g, 4.15 mmol) was dissolved in dry DCM (10 mL) and stirred in an ice bath. Then, N-hydroxysuccinimide (NHS, 0.72 g, 6.22 mmol) and N, N'-dicyclohexylcarbodiimide (DCC, 1.20 g, 5.81 mmol) were slowly added to the stirring solution. The crude was allowed to warm to room temperature and left to stir for another 1 hour. The oil-like product **A5** (2.10 g, 3.48 mmol) was re-dissolved in dry DCM (10 mL) and added to the stirring solution together with triethyl amine (1.15 mL, 8.30 mmol). The crude was left to stir overnight at room temperature. After the reaction was complete (as determined by TLC), the reaction mixture was transferred to a separatory funnel and diluted with water (50 mL) and DCM (50 mL). The aqueous fraction was extracted with DCM (2 x 50 mL). The combined organic layer was dried with Na_2SO_4. The Na_2SO_4 was filtered off and the solvent was removed *in vacuo*. The crude product was further purified by silica column chromatography using PE/EtOAc solvent gradient (4:1 to 1:1, v:v). The yellow oil-like product **A7** was obtained by evaporating the solvent *in vacuo*.

Yield: 1.80 g, 69%. ^{1}H-NMR ($CDCl_3$, 400 MHz): 7.52-7.49 (m,6H), 7.30-7.26 (m, 6H), 7.20-7.16 (m, 3H), 6.74 (br s, 1H), 5.20 (br s, 1H), 4.24-4.22 (m, 2H), 3.70-3.47 (m, 16H), 3.18-3.13 (m, 2H), 3.01-2.98 (m, 2H), 2.30 (br s, 1H), 2.16-2.12 (m, 2H), 1.49 (s, 3H), 1.35-1.25 (m, 12H). ^{13}C-NMR ($CDCl_3$, 100 MHz): 174.71, 156.58, 146.49, 129.17, 127.86, 126.27, 70.98, 70.75, 70.68, 70.62, 70.36, 69.86, 69.70, 63.85, 57.13, 49.45, 43.68, 41.19, 39.92, 30.98, 30.08, 29.68, 29.39, 27.44, 26.88, 24.12.

Synthesis of compound A8

Compound **A7** (1.22 g, 1.62 mmol) was dissolved in trifluoroacetic acid (TFA, 15 mL) and was left to stir for 3 h at room temperature. Completion of the reaction was confirmed by TLC analysis and the remaining TFA was evaporated by a gentle stream of air. The crude was redissolved in chloroform (20 mL), followed by the addition of 3,4-dibutoxy-3-cyclobutene-1,2-dione (420 µL, 1.94 mmol) and DIPEA (564 µL, 3.24 mmol). The mixture solution was left to stir overnight at room temperature. The reaction mixture was transferred to a separatory funnel after confirming its completion using LC-MS and diluted with water (50 mL) and DCM (50 mL). The aqueous fraction was extracted with DCM (2 x 50 mL) and the

combined organic layers were dried with Na_2SO_4. The Na_2SO_4 was filtered off and the solvent was removed *in vacuo*. The crude product was further purified by silica column chromatography using a solvent gradient from PE/EtOAc (2:1, v:v) to pure EtOAc. The oil-like product **A8** was obtained by evaporating the solvent *in vacuo*.

Yield: 0.72 g, 67%. ^{1}H-NMR ($CDCl_3$, 400 MHz): 7.52-7.48 (m, 1H), 6.78-6.75 (m, 1H), 5.25-5.17 (m, 1H), 4.56-4.46 (m, 2H), 4.03-3.93 (m, 2H), 3.49-3.37 (m, 14H), 3.29-3.21 (m, 4H), 2.97-2.92 (m, 2H), 2.82-2.79 (m, 2H), 1.64-1.05 (m, 19H), 0.81-0.74 (m, 3H). ^{13}C-NMR ($CDCl_3$, 100 MHz): 189.03, 182.44, 176.74, 174.24, 156.17, 72.84, 70.12, 70.05, 69.76, 69.21, 69.04, 63.33, 60.00, 56.73, 48.62, 44.43, 44.24, 40.57, 39.37, 31.60, 30.19, 29.45, 28.70, 28.64, 26.23, 23.69, 18.26, 13.19. LC-MS: t = 7.41min, m/z: 662.27 $[M+H]^+$, calc: 661.31.

Synthesis of compound SQ-DT

Component **A8** (0.41 g, 0.63 mmol) was dissolved in chloroform (20 mL), followed by adding tris(2-aminoethyl)amine (28 µL, 0.19 mmol) and DIPEA (110 µL, 0.63 mmol). The resulting crude was left to reflux overnight. After the reaction was complete (as determined by LC-MS), the crude was first purified by silica column chromatography using a gradient from pure EtOAc to EtOAc/MeOH (4:1, v:v). The compound was further purified by HPLC with UV detection and lyophilized to obtain a white solid **SQ-DT**.

Yield: 0.15 g, 42%. ^{1}H-NMR (DMSO-d_6, 400 MHz): 7.93-7.91 (m, 3H), 7.48 -7.27 (m, 6H), 7.19-7.15 (m, 3H), 4.04-4.01 (m, 6H), 3.56-3.40 (m, 52H), 3.26-3.20 (m, 8H), 3.00-2.90 (m, 12H), 2.72-2.69 (m, 6H), 1.49-1.21 (m, 45H). ^{13}C-NMR (DMSO-d_6, 100 MHz): 182.85, 173.63, 167.94, 156.57, 70.20, 70.08, 69.37, 69.18, 63.42, 57.57, 47.66, 43.76, 31.18, 29.85, 29.15, 26.69, 26.32, 24.05, 23.93. LC-MS: t = 6.92 min, m/z: 1909.67 $[M+H]^+$; HR-MS (ESI) m/z: 955.4350 $[M+2H]^+/2$, $C_{84}H_{141}N_{13}O_{24}S_6$.

Synthesis of monomer SQ-RGD

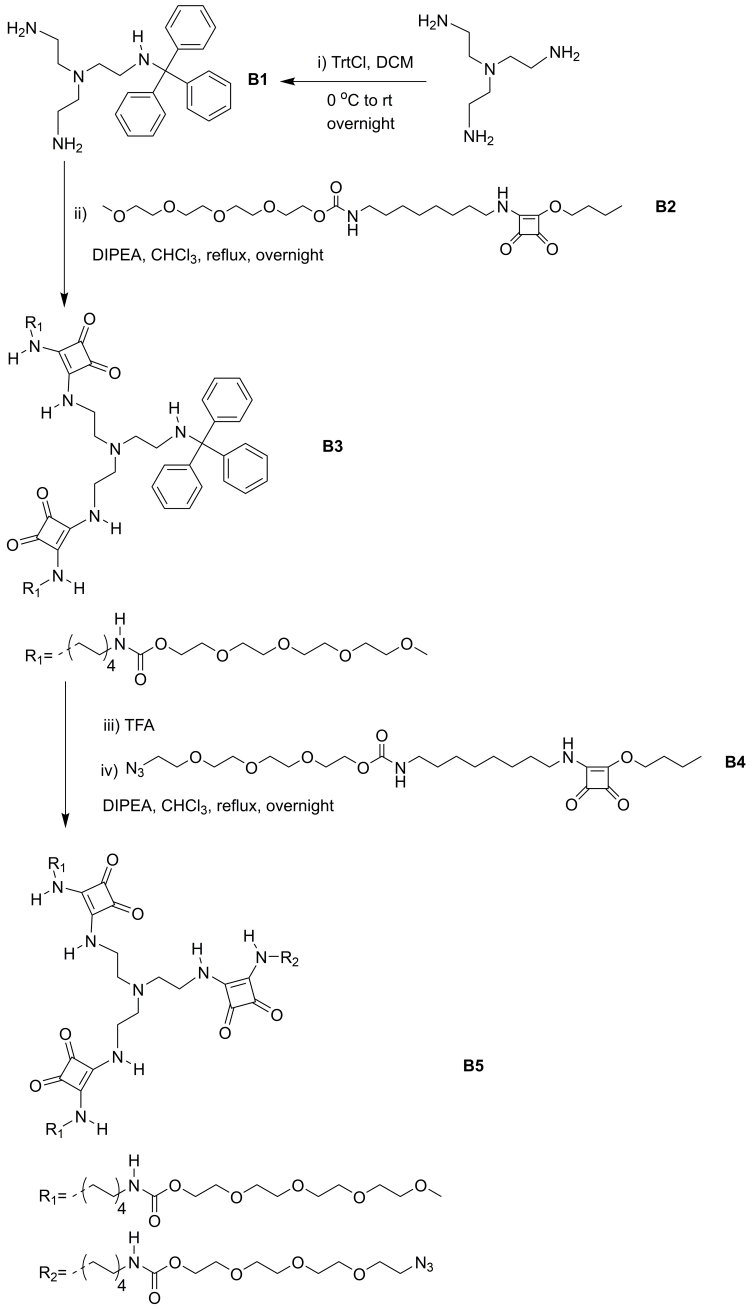

Scheme S3.2 Synthetic route of monomer **SQ-A** (**B5**).

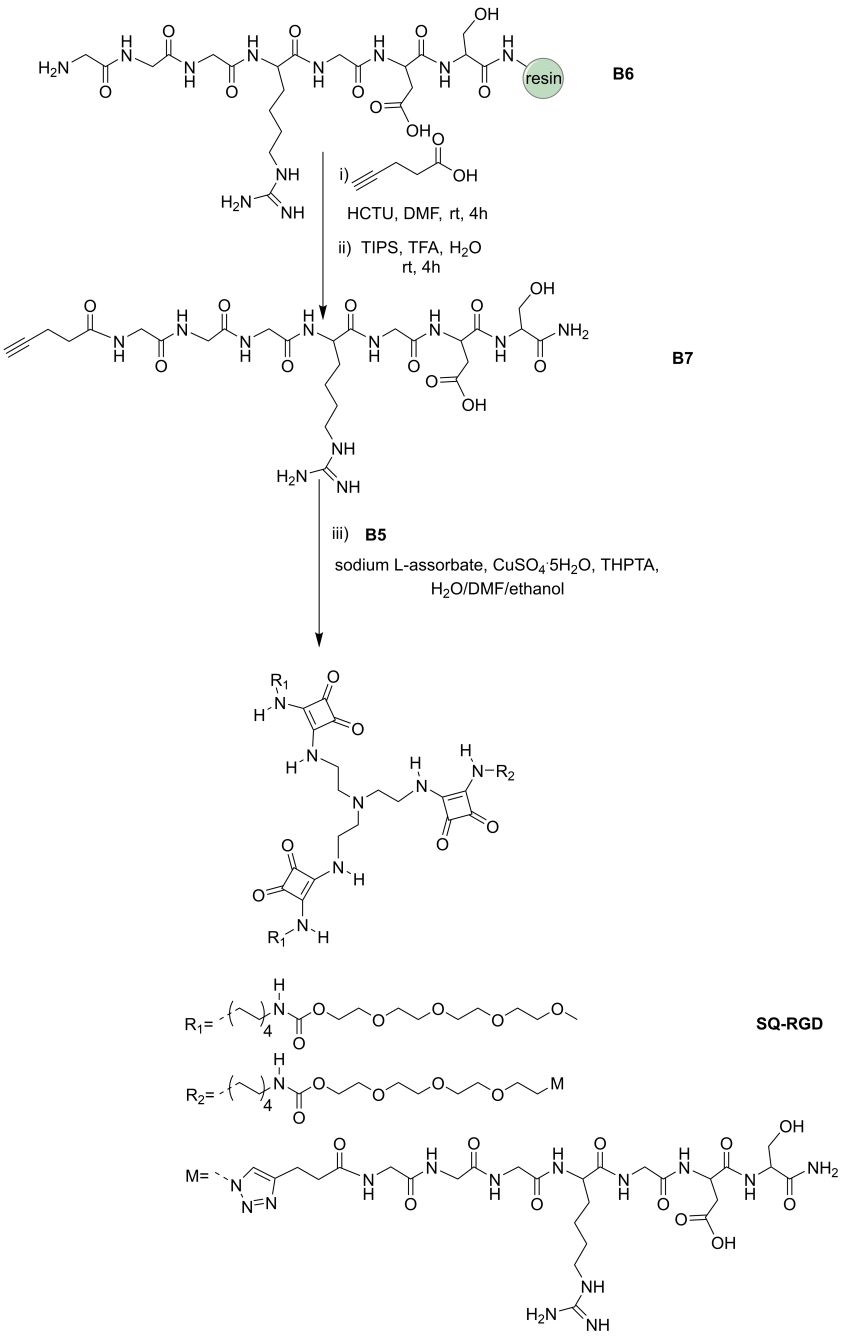

Scheme S3.3 Synthetic route of monomer **SQ-RGD**.

Synthesis of compound B1

Tris(2-aminoethyl)amine (5 mL, 33.37 mmol) was dissolved in DCM (200 mL) and the resulting solution was stirred in an ice bath. Trityl chloride (0.93 g, 3.34 mmol) in DCM (100 mL) was added dropwise to the stirring solution over 2 hours. The reaction mixture was allowed to further stir overnight at room temperature. After the reaction was complete (as determined by TLC), the solution was concentrated by rotary evaporation and EtOAc (100 mL) was added. The crude was washed with water (3 x 100 mL) and the aqueous layers were discarded. The combined organic layer was dried over Na_2SO_4 and the solvent was removed under vacuum to obtain the colorless oil-like product **B1** without further purification.

Yield: 1.23 g, 95 %. ^{1}H-NMR ($CDCl_3$, 400 MHz): 7.55-7.51 (m, 6H), 7.49-7.28 (m, 6H), 7.25-7.19 (m, 3H), 2.72-2.60 (m, 4H), 2.44-2.26 (m, 2H), 2.38-2.35 (m, 4H), 2.29-2.26 (m, 2H). ^{13}C-NMR ($CDCl_3$, 100 MHz): 146.57, 128.94, 128.16, 126.59, 70.98, 58.11, 55.36, 41.27, 40.37.

Synthesis of compound B3

Component **B2** (1.21 g, 2.28 mmol) was synthesized according as previously reported,[1] and dissolved in chloroform (20 mL), followed by the addition of **B1** (402 mg, 1.03 mmol) and DIPEA (397 µL, 2.28 mmol). The reaction mixture was refluxed overnight. After the reaction was complete (as determined by LC-MS), the mixture was transferred to a separatory funnel and diluted with DCM (100 mL) and water (100 mL). The organic layer was collected, and the aqueous layer was further extracted with DCM (2 x 100 mL). The combined organic layers were dried with Na_2SO_4. The Na_2SO_4 was filtered, and the solvent was removed by rotary evaporation *in vacuo*. The obtained crude was purified by silica column chromatography using a gradient from pure EtOAc to EtOAc/MeOH (4:1, v:v). The solvent was evaporated *in vacuo* to provide the oil-like product **B3**.

Yield: 0.65 g, 49%. ^{1}H-NMR ($CDCl_3$, 400 MHz): 7.44-7.40 (m, 6H), 7.34-7.27 (m, 6H), 7.24-7.11 (m, 3H), 5.05-5.01 (m, 2H), 4.23-4.20 (m, 4H), 3.71-3.55 (m, 36H), 3.39 (s, 6H), 3.21-3.10 (m, 4H), 2.60-2.42 (m, 6H), 2.23-2.20 (m, 2H), 1.68-1.28 (m, 24H). ^{13}C-NMR ($CDCl_3$, 100 MHz): 182.90, 172.52, 146.12, 128.47, 127.78, 126.15, 71.89, 70.39, 69.65, 69.29, 63.76, 59.01, 44.75, 40.97, 30.93, 29.89, 29.15, 26.69, 26.46.

Synthesis of compound B4

Compound **A4** (1.02 g, 1.64 mmol) was dissolved in TFA (10 mL) and was left to stir for 3h at room temperature. Completion of the reaction was confirmed by TLC and TFA was then removed by using a gentle stream of air. The crude was redissolved in chloroform (30 mL), followed by the addition of 3,4-dibutoxy-3-cyclobutene-1,2-dione (425 µL, 1.97 mmol) and DIPEA (571 µL, 3.28 mmol). The reaction mixture was left to stir overnight at room temperature. After the reaction was complete (as determined by TLC), the mixture was transferred to a separatory funnel and diluted with water (100 mL) and DCM (100 mL). The aqueous fraction was extracted with DCM (2 x 100 mL). The combined organic layers were dried with Na_2SO_4. The Na_2SO_4 was filtered off and the solvent was removed *in vacuo*. The crude product was further purified by silica column chromatography using a gradient from PE/EtOAc (2:1, v:v) to pure EtOAc. The oil-like product **B4** was obtained by evaporating the solvent *in vacuo*.

Yield: 0.54 g, 61%. ^{1}H-NMR ($CDCl_3$, 400 MHz): 7.17-7.13 (m, 1H), 4.93-4.90 (m, 1H), 4.68-4.61 (m, 2H), 4.20-4.15 (m, 2H), 3.65-3.62 (m, 12H), 3.40-3.33 (m, 2H), 3.13-3.08 (m, 2H), 1.76-1.26 (m, 18H), 0.94-0.91 (m, 3H). ^{13}C-NMR ($CDCl_3$, 100 MHz): 189.70, 182.69, 177.54, 172.93, 172.43, 156.50, 73.44, 70.67, 70.64, 70.61, 70.50, 70.04, 69.65, 64.44, 63.85, 50.68, 44.87, 41.64, 40.96, 32.01, 30.98, 30.57, 29.85, 29.06, 28.99, 26.58, 26.28, 18.65, 13.68.

Synthesis of compound SQ-A (B5)

Compound **B3** (0.51 g, 0.39 mmol) was dissolved in TFA (10 mL) and was left to stir for 2h at the room temperature. Completion of the reaction was confirmed by TLC and the remaining TFA was removed by a gentle stream of air. The crude was redissolved in chloroform (30 mL), followed by the addition of **B4** (0.25 g, 0.46 mmol) and DIPEA (135 µL, 0.78 mmol). The reaction mixture was left to reflux overnight. After the reaction was complete (as detected by LC-MS), the mixture was transferred to a separatory funnel and diluted with water (100 mL) and DCM (100 mL). The aqueous fraction was extracted with DCM (2 x 100 mL) and the combined organic layers were dried with Na_2SO_4 and filtered. The solvent was removed *in vacuo*. The crude product was purified by silica column chromatography using a solvent gradient from pure EtOAc to EtOAc/MeOH (4:1, v:v). The product was further purified by reverse phase silica column

chromatography on a C18 silica gel column using a gradient of CH_3CN/H_2O (1:9 to 9:1, v:v) over 41 minutes. The product was lyophilized overnight to obtain a white solid **SQ-N_3** (**B5**).

Yield: 0.24 g, 40%. ^{1}H-NMR ($CDCl_3$, 400 MHz): 7.46 (br s, 2H), 7.28 (br s, 2H), 7.16 (br s, 2H), 4.04-4.00 (m, 6H), 3.60-3.37 (m, 52H), 3.22 (s, 6H), 2.95-2.90 (m, 6H), 2.70-2.68 (m, 6H), 1.50-1.21 (m, 38H). ^{13}C-NMR ($CDCl_3$, 100 MHz): 181.75, 181.54, 167.38, 166.83, 155.47, 70.61, 69.15, 69.11, 69.06, 69.03, 68.92, 68.60, 68.24, 62.32, 57.38, 54.07, 49.33, 42.64, 40.90, 39,52, 30.05, 28.72, 28.03, 27.96, 25.56, 25.19. LC-MS: t = 5.49 min, m/z: 1527.67 $[M+H]^+$, calc: 1525.89.

Synthesis of peptide RGD and DGR

The peptide **RGD** (**GGGRGDS**) and **DGR** (**GGGDGRS**) were synthesized by standard Fmoc solid-phase peptide synthesis (SPPS) on resin at room temperature. Using the synthesis of the **RGD** peptide **GGGRGDS** (**B6**, 0.5 mmol) an example, the resin (0.68 g, 0.74 mmol/g) was first swollen in N,N-dimethylformamide (DMF, 8 mL) for 30 min, followed by deprotecting the Fmoc groups of the resin via piperidine in DMF (20%, v/v, 8 mL) for 1h with shaking. The resin was washed with DMF (5 x 8 mL) and then functionalized with the first Fmoc amino acid (2.0 eq.) by shaking for 4h with HCTU (3.0 eq.), and DIPEA (5.0 eq.) in DMF (8 mL). Then, the resin was washed with DMF (5 x 8 mL), followed by deprotection of the Fmoc of amino acid with piperidine in DMF (20%, v/v, 8 mL) by shaking for another 30 min. Subsequently, the following amino acid couplings were performed according to the same protocol as the first amino acid coupling. Once the coupling of the last Fmoc of amino acid was finished, its deprotection was performed using piperidine in DMF (20%, v/v, 8 mL) with 30 min shaking and was further washed with DMF (5 x 8 mL). The peptide was cleaved from the resin using a mixture of TFA:TIPS:water (95:2.5:2.5, v:v:v, 1 mL) with 4h shaking at room temperature. Then, the crude peptide was precipitated from cold diethyl ether, collected by centrifugation, and re-dissolved in water. The peptide **B6** was detected and confirmed by LC-MS. The remaining **RGD** peptide on the resin (**GGGRGDS**) was stored at -20 °C before use.

The control sequence peptide **DGR** (**GGGDGRS**) that is unable to bind to cell surface integrins was synthesized according to the same procedure as the **RGD** peptide mentioned above.

Synthesis of alkyne-functionalized RGD peptide B7

The **GGGRGDS** (**B6)** peptide on the resin (0.25 mmol) was further functionalized with 4-pentynoic acid (2.0 eq.) by shaking together with HCTU (3.0 eq.) and DIPEA (5.0 eq.) in DMF (8 mL) for 6 h. The peptide was then cleaved from the resin after confirmation of the reaction was complete by LC-MS using TFA:TIPS:water (95:2.5:2.5, v:v:v, 8 mL) and 6h shaking. The peptide was precipitated using cold diethyl ether, collected by centrifugation and re-dissolved in water. **B7** was confirmed by LC-MS and without any other further purification was then lyophilized overnight. The obtained peptide was stored at -20 °C before use. LC-MS: t = 1.02 min, m/z: 684.28 $[M+H]^+$, calc: 683.30.

Synthesis of compound SQ-RGD

The alkyne-functionalized peptide **B7** was coupled to azide-based compound **B5** through copper(I)-catalyzed azide-alkyne cycloaddition (CuAAc). Firstly, sodium L-ascorbate (52.69 mg, 265.98 µmol) and copper (II) sulfate pentahydrate (8.85 mg, 35.46 µmol) were separately dissolved in 139 µL H_2O by vortexing. Then, a homogeneous bright yellow solution was obtained by mixing the above two solutions with 60s vortexing. Tris(3-hydroxypropyltriazolylmethyl) amine (THPTA, 7.7 mg, 17.73 µmol) dissolved in ethanol (280 µL), and compound **B5** (67.64 mg, 44.33 µmol) dissolved in DMF (1.7 mL) were mixed in 10 mL flask, followed by the addition of the pre-prepared yellow solution above. Finally, peptide **B7** (56.42 mg, 82.49 µmol) dissolved in 320 µL DMF and 320 µL H_2O was added into the reaction mixture and stirred at room temperature for 4h under N_2 gas. After the reaction was complete as determined by LC-MS, the crude was first dialyzed against water (cut off Mw 500-1000 Da) for two days at room temperature and further purified by HPLC. The white powder product **SQ-RGD** was obtained through overnight lyophilization and was stored at -20 ^{0}C before use. LC-MS: t = 5.24 min, m/z: 1106.13 $[M+2H^+]/2$; HR-MS (ESI) m/z: 737.7365 $[M+3H^+]/3$, $C_{97}H_{164}N_{24}O_{34}$.

Synthesis of 1,2-dithiolane functioned peptides (DT-RGD and DT-DGR)

To obtain RGD-peptides end-functionalized with the 1,2-dithiolane group, e.g., **DT-RGD** (**(DT)GGGRGDS**) and **DT-DGR** (**(DT)GGGDGRS**), the peptide **RGD** and **DGR** were separately functionalized with the 1,2-dithiolane **A6** (2.0 eq.) on resin by shaking in combination with HCTU (3.0 eq.) and DIPEA (5.0 eq.) in DMF (8 mL) overnight. After the reaction, the peptide containing resin was washed with DMF

(5 x 8 mL), and cleaved with TFA:TIPS:water (95:2.5:2.5, v:v:v, 8 mL) over 4 h with shaking. The crude peptide was precipitated using cold diethyl ether, collected by centrifugation and re-dissolved in water. The peptide was further purified by HPLC and the white powder was obtained by overnight lyophilization. The obtained peptides **DT-RGD** and **DT-DGR** were stored at -20 °C before use. HR-MS (ESI) m/z: 750.2656 [M+H$^+$], $C_{26}H_{43}N_{11}O_{11}S_2$.

3.6.3 Multicomponent hydrogels preparation and gel inversion experiments

The stock solutions (10.0 mM) of **SQ** and **SQ-DT** were separately prepared by dissolving each monomer in DMSO with 2 min vortexing. To obtain the different multicomponent hydrogel systems, namely **SQ/xSQ-DT** (x: molar percent of **SQ-DT** of the total monomer concentration), the required volume of each monomer stock solution was pipetted into the glass vials (2.0 mL) with 30 s of gentle vortexing. The DMSO was removed using a stream of the N_2 overnight to obtain dried films with the mixed monomers and were further freeze-dried overnight to completely remove the DMSO. Then, PBS (pH 7.4, 500-1000 µL) was added and sonicated for 20-60 min (depend on the power of the sonication bath and also the concentration of total monomer) in an ice bath (~4 °C) to obtain optically clear solutions. These solutions were then incubated at 37 °C in an oven for 15 min to allow gelation to occur. The transparent hydrogels were further equilibrated at room temperature overnight prior to performing further experiments.

The preparation of the multicomponent hydrogel **SQ/xSQ-DT/ySQ-RGD** (x and y: molar percent of **SQ-DT** and **SQ-RGD** of the total monomer concentration) followed the same procedure as mentioned above.

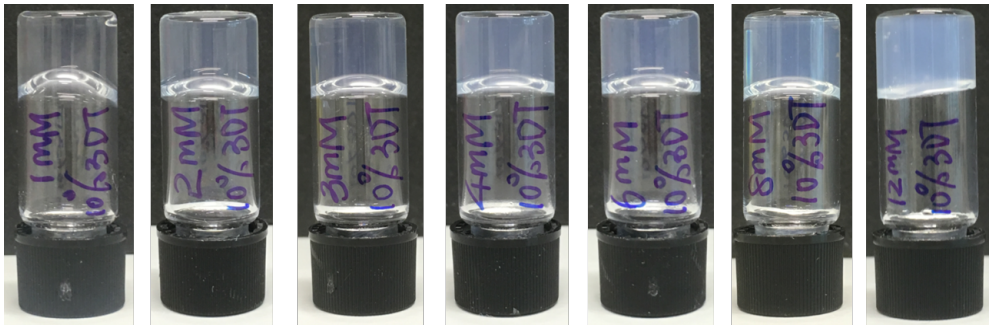

Figure S3.1 Gel inversion test of multicomponent squaramide-based supramolecular hydrogels (**SQ/10SQ-DT**) with varied total monomer concentrations (1.0-12.0 mM) in PBS (pH 7.4) after overnight equilibration at room temperature.

3.6.4 Oscillatory rheology

The pre-made hydrogels after overnight equilibration (as mentioned above) were gently pipetted on to 20 mm quartz plate. The gap was set to 300 µm. Before data collection, the samples loaded in the plates were equilibrated for 5 min to allow the hydrogels to self-recover to their initial state. After time sweep experiment for 60s, the hydrogels were further stiffened by turning on the light through the Excelitas Omnicure S2000 system (wavelength: 320-500 nm, primary peak: 365 nm). All time sweep measurements were performed with 0.05% strain (γ) at a frequency (f) of 1.0 Hz. Frequency sweeps were conducted in the range of 0.01-10.0 Hz at a constant strain of 0.05%. Strain sweeps were performed in the range of 0.01-500% at a fixed frequency (1.0 Hz). To measure their self-recovery properties before and after UV light irradiation, a time-dependent recovery measurement was performed using a low strain of 0.05% (f = 1.0 Hz) for 120 s after a strain experiment. Once the storage modulus (G') was reached a plateau, a higher strain of 300% was applied for another 120s to break the hydrogels and was continued with a time sweep at low strain 0.05% (f = 1.0 Hz). These self-recovery experiments were alternated in this manner for two cycles.

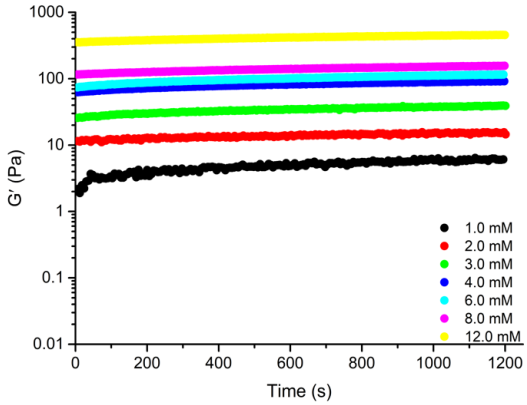

Figure S3.2 Averaged (N = 3) time sweep measurements of **SQ/10SQ-DT** with different total monomer concentrations without UV light irradiation at the fixed strain (γ = 0.05%) and frequency (f = 1.0 Hz) at the room temperature.

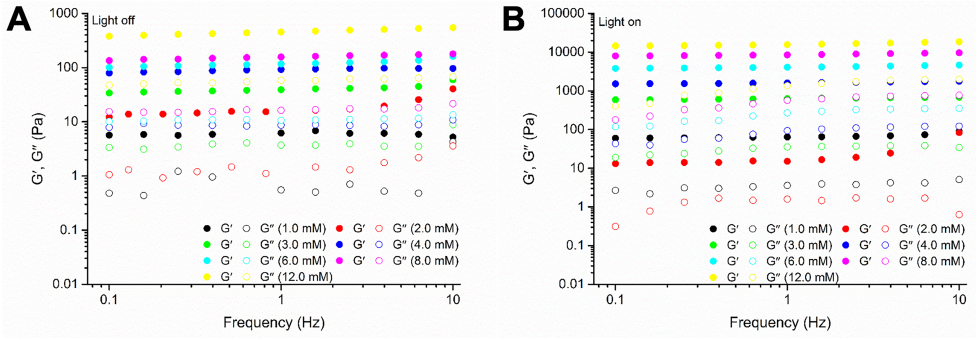

Figure S3.3 Averaged (N ≥ 3) frequency sweep (from 0.1 to 10 Hz) of **SQ/10SQ-DT** with different total monomer concentrations (A) without and (B) with 10 min UV light irradiation (~10.0 mW/cm^2, 320-500 nm with a primary peak at 365 nm) at a fixed strain (γ = 0.05%) at the room temperature.

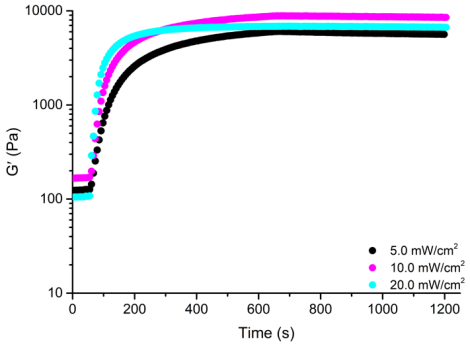

Figure S3.4 Averaged (N = 3) time sweep of **SQ/10SQ-DT** (8.0 mM) with 10 min UV light irradiation (320-500 nm with maximum absorbance at 365 nm) using different light intensities (~5 mW/cm^2, ~10 mW/cm^2, and ~20 mW/cm^2) at the room temperature at a fixed strain (γ = 0.05%) and frequency (f = 1.0 Hz).

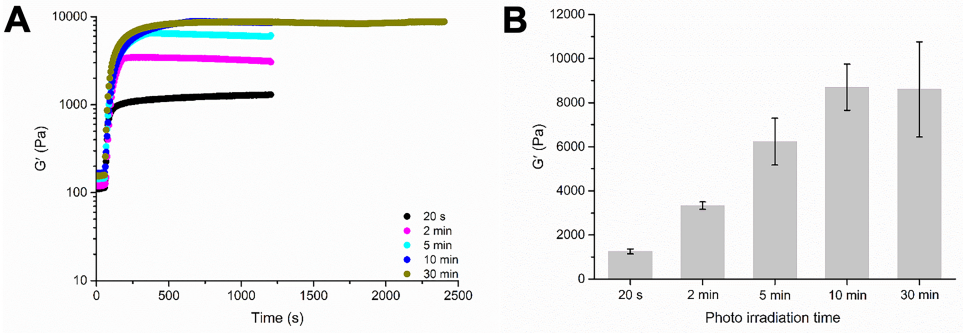

Figure S3.5 Averaged (N = 3) (A) time sweep and (B) plateau storage moduli (G´) at a fixed strain (γ = 0.05%) and frequency (f = 1.0 Hz) of **SQ/10SQ-DT** (8.0 mM) with different UV light irradiation times (20 s, 2 min, 5 min, 10 min and 30 min) at room temperature (~10 mW/cm^2, 320-500 nm with maximum absorbance at 365 nm). Error bars were calculated according to the average of repeat measurements (N = 3).

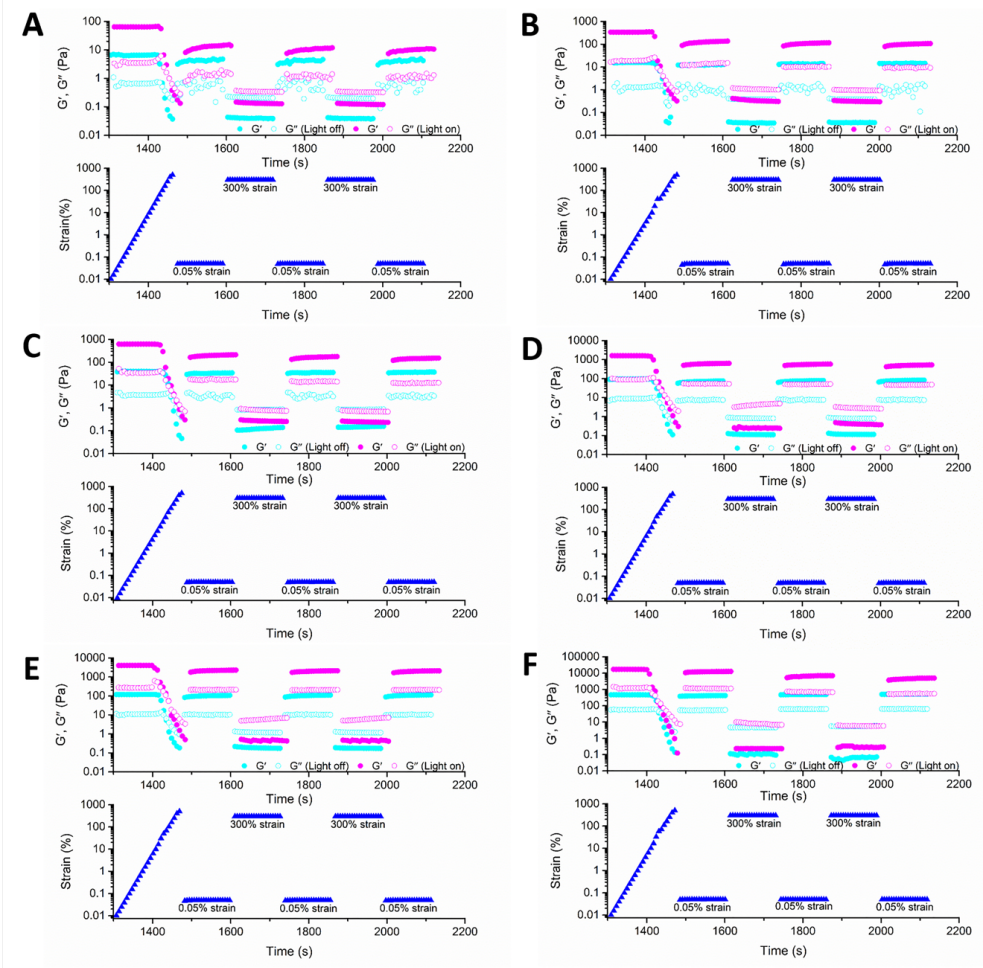

Figure S3.6 Averaged (N ≥ 3) strain sweep experiment and step-strain experiment of hydrogel system (**SQ/10SQ-DT**) without and with 10 min light irradiation (~10 mW/cm^2, 320-500 nm with a primary peak at 365 nm) at a fixed frequency (f = 1.0 Hz) at room temperature with different total monomer concentrations: (A) 1.0 mM; (B) 2.0 mM; (C) 3.0 mM; (D) 4.0 mM; (E) 6.0 mM and (F) 12.0 mM.

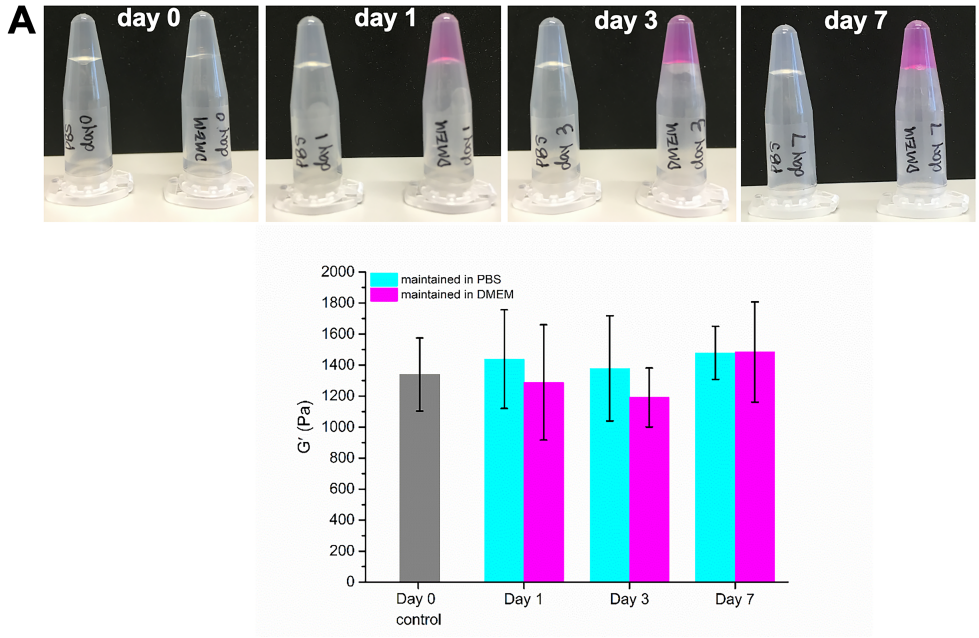

Figure S3.7 (A) Representative gel inversion tests and (B) the averaged (N = 2) plateau storage moduli (G´) of the stiffened **SQ/10SQ-DT** (4.0 mM) hydrogels using UV light irradiation (10 min, ~10 mW/cm², 320-500 nm with maximum absorbance at 365 nm) before and after maintenance in PBS (pH 7.4) or cell culture medium DMEM containing 20% serum at 37°C for different time points (e.g., day 1, 3 and 7). The PBS and DMEM medium were changed every day during the maintenance. Error bars were calculated according to the average of repeat measurements (N = 2).

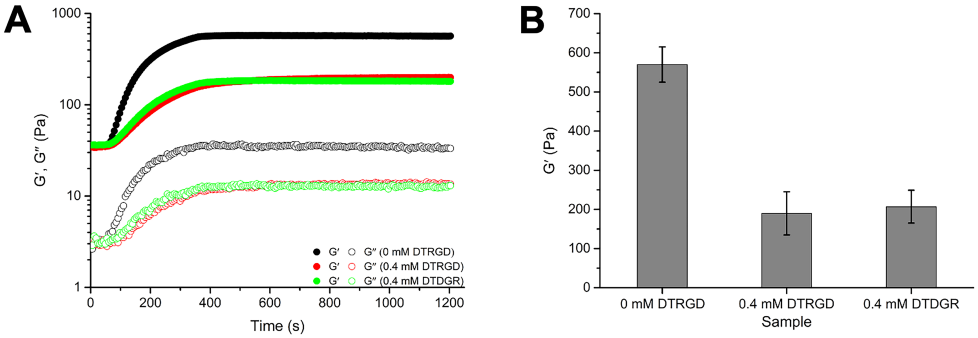

Figure S3.8 Averaged (N = 3) (A) time sweep and (B) plateau storage moduli (G´) at a fixed strain (γ = 0.05%) and frequency (f = 1.0 Hz) of hydrogel system **SQ/10SQ-DT** (3.0 mM) without adding peptide or with peptide **DT-RGD** (0.4 mM) or **DT-DGR** (0.4 mM) with 5 min UV irradiation at room temperature (~10 mW/cm², 320-500 nm with maximum absorbance at 365 nm). Error bars were calculated according to the average of repeat measurements (N = 3).

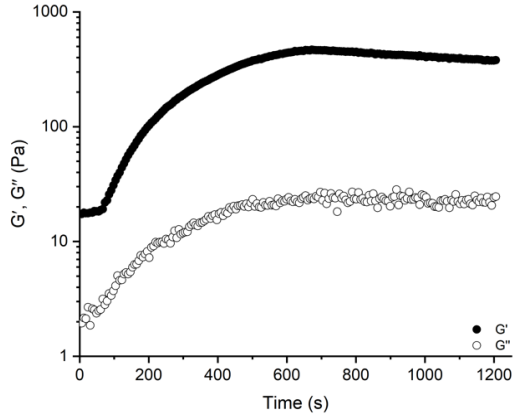

Figure S3.9 Average (N = 2) time sweep experiment of **SQ/10SQ-DT/10SQ-RGD** (4.0 mM) hydrogel with 5 min UV irradiation (~10 mW/cm^2, 320-500 nm with maximum absorbance at 365 nm) at a fixed strain (γ = 0.05%) and frequency (f = 1.0 Hz) at room temperature.

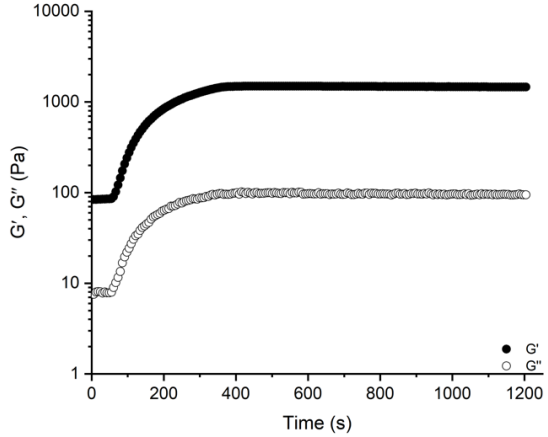

Figure S3.10 Average (N = 3) time sweep experiment of **SQ/10SQ-DT/3.4SQ-RGD** (6.0 mM) with 5 min UV irradiation (~10.0 mW/cm^2, 320-500 nm with maximum absorbance at 365 nm) at a fixed strain (γ = 0.05%) and frequency (f = 1.0 Hz) at room temperature.

3.6.5 Ellman's assay study

Calibration curve for Ellman's assay

The calibration curve for Ellman's test was prepared using DL-Dithiothreitol (DTT) as the control. Firstly, the stock solutions of DTT (5.0 mM) and 5,5'-dithiobis-(2-nitrobenzoic acid) (DTNB) (1.8 mM) were separately prepared in phosphate buffer (10 mM, pH~8). The DTT stock solution (5.0 mM) was further diluted with

phosphate buffer to different concentrations (e.g., from 0.1-1.9 mM with 0.2 mM increments). Then, the DTNB stock solution (1.8 mM, 25 µL) was independently reacted with the pre-made DTT solutions (25 µL) above for 10 min. Finally, prior to UV-Vis measurements, each solution after reaction was further diluted with phosphate buffer (950 µL) resulting in the same DTNB (45 µM) and varied DTT (e.g., 0 µM, 2.5 µM, 7.5 µM, 12.5 µM, 17.5 µM, 22.5 µM, 27.5 µM, 32.5 µM, 37.5 µM, 42.5 µM and 47.5 µM) concentrations. The UV-Vis spectrum of each diluted solution was then collected at room temperature (**Figure S3.11A**) and the related standard calibration curve for the Ellman's assay was plotted based on the absorbance at 412 nm (**Figure S3.11B**). The obtained equation for the standard calibration curve: $Abs_{412\ nm}$ = 0.02686x (µM) + 0.00844.

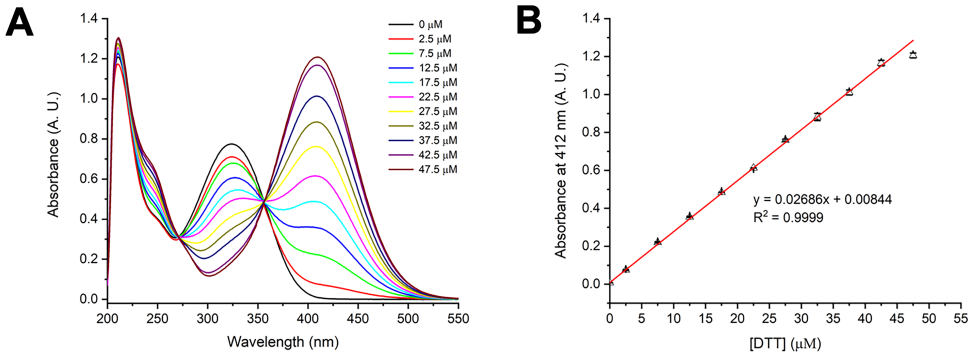

Figure S3.11 (A) UV-Vis spectra of the diluted reaction solutions containing the same concentration of DTNB (45 µM) and increasing concentrations of DTT (0-47.5 µM) in phosphate buffer (pH 8.0) at room temperature. (B) The plotted calibration curve for Ellman's assay using DTT as a control based on the absorbance at 412 nm obtained from UV-Vis spectra.

Ellman's assay on supramolecular polymer solutions and hydrogels before and after UV irradiation

The pre-gel solutions of **SQ/10SQ-DT** (4.0 mM) in PBS (pH 7.4) after sonication in an ice bath were either directly (4.0 mM, 500 µL) pipetted or further diluted with PBS (pH 7.4) to a lower concentration (0.4 mM, 500 µL) before pipetting into new glass vials (2.0 mL). Both samples were equilibrated at 37°C for 15 min and equilibrated overnight at room temperature to form supramolecular polymers (0.4 mM) or hydrogels (4.0 mM). The samples for each concentration were aliquoted into three independent glass vials (100 µL each) to further explore the effect of the different light irradiation times in the following studies.

The three vials containing the solution **SQ/10SQ-DT** (0.4 mM) above were UV irradiated at different times (0 min, 5 min and 10 min) using a benchtop LED source (~10.0 mW/cm^2, 375 nm). The samples (0.4 mM, 25 µL) were then pipetted out to react with the DTNB stock solution (1.8 mM, 25 µL) at room temperature for 10 min. The samples were further diluted with phosphate buffer (950 µL) prior to UV-Vis measurements to provide **SQ/10SQ-DT** (0.1 mM) and DTNB (45 µM).

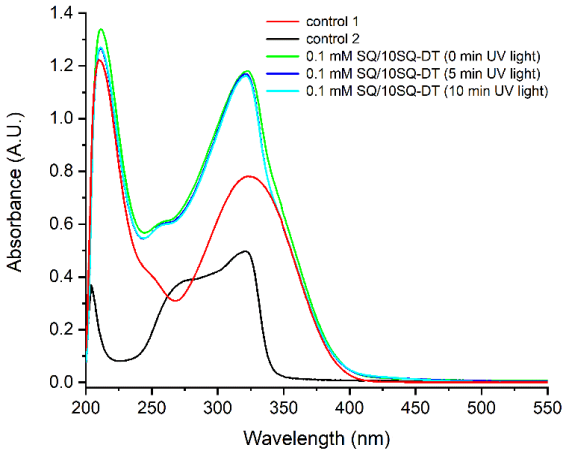

Figure S3.12 UV-Vis spectra at room temperature of Ellman's test on **SQ/10SQ-DT** solutions. The diluted reaction solutions containing the same concentration of DTNB (45 µM) and the various supramolecular polymer solutions (0.1 mM **SQ/10SQ-DT**) applied with different UV irradiation time (0 min, 5 min and 10 min) using a benchtop LED source (~10 mW/cm^2, 375 nm). Control 1: supramolecular polymer solution (0.1 mM **SQ/10SQ-DT**) before reacting with the DTNB solution; control 2: DTNB solution (45 µM) before reacting with the supramolecular polymer solutions.

Prior to the Ellman's test on hydrogels, the three vials containing hydrogels **SQ/10SQ-DT** (4.0 mM) were irradiated with UV light at different times (0 min, 5 min and 10 min) using a benchtop LED source (~10.0 mW/cm^2, 375 nm) source. An aliquot of the DTNB stock solution (1.8 mM, 600 µL) was then applied on top of the hydrogels at room temperature for 10 min. After reaction, an aliquot of the supernatant (25 µL) was removed and further diluted with phosphate buffer (975 µL) before UV-Vis analysis at room temperature.

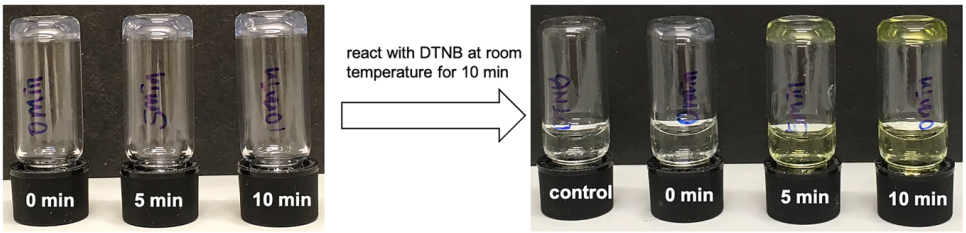

Figure S3.13 Photographs of **SQ/10SQ-DT** (4.0 mM) hydrogels. Samples are first prepared with different UV irradiation times (0 min, 5 min and 10 min) using a benchtop LED source (~10.0 mW/cm^2, 375 nm) (*left*). After reaction with the DTNB stock solution (1.8 mM, 600 µL) at room temperature for 10 min and a control of the DTNB solution (1.8 mM) without any gel material (*right*).

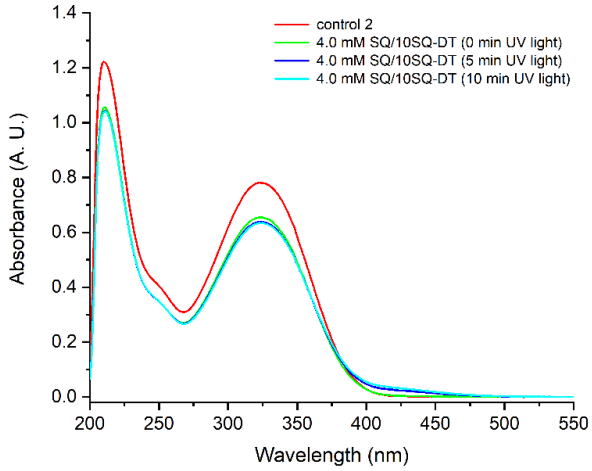

Figure S3.14 UV-Vis spectra at room temperature of Ellman's test on **SQ/10SQ-DT** gels. The diluted reaction solutions of the supernatant (1.8 mM) from top of various supramolecular hydrogels (4.0 mM **SQ/10SQ-DT**) with the application of different UV irradiation time (0 min, 5 min and 10 min) using a benchtop LED source (~10 mW/cm^2, 375 nm). Control 2: the pure DTNB solution (45 µM) before reacting with gel materials.

Table S3.1 Average (N = 2) absorbance at 412 nm for the various Ellman's test samples.

Samples	Control 1	Control 2	Solution 1	Solution 2	Solution 3	Gel 1	Gel 2	Gel 3
UV irradiation (min)	0	0	0	5	10	0	5	10
Averaged absorbance at 412 nm	0.0084 ± 0.00035	0.0047 ± 0.0026	0.0016 ± 0.0058	0.023 ± 0.0036	0.026 ± 0.0053	0.0084 ± 0.00086	0.021 ± 0.0069	0.032 ± 0.0087

Control 1: 0.1 mM **SQ/10SQ-DT** with 0 μM DTNB; Control 2: 45 μM DTNB; Solution 1-3: 0.1 mM **SQ/10SQ-DT** with 45 μM DTNB; Gel 1-3: 4.0 mM **SQ/10SQ-DT** with 45 μM DTNB. UV irradiation was applied using a benchtop LED source (~10 mW/cm^2, 375 nm).

3.6.6 Cryogenic-Transmission Electron Microscopy (Cryo-TEM)

The multicomponent hydrogels **SQ/10SQ-DT** (2.0 mM) were first prepared and equilibrated overnight before use. Then hydrogel (100 μL) was pipetted into a new glass vial (2.0 mL) and UV irradiation was applied for 10 min using a benchtop LED source (~10 mW/cm^2, 375 nm) at room temperature. After that, hydrogel samples (3 μL) for each UV irradiation time (0 min and 10 min) were separately pipetted without further dilution onto freshly glow-discharged copper grids, and the excess liquid was blotted away for 2 s using Whatman No. 4 filter paper (98% humidity) and plunge-frozen in a mixture liquid ethane and propane at -196 °C using a Leica EM GP (Leica Microsystems). The Cryo-TEM samples were stored in liquid nitrogen before imaging. The Cryo-TEM images of samples were collected on a Tecnai F12 microscope (FEI) (see **Figure 3.3A, B**).

3.6.7 Small angle X-ray scattering (SAXS)

Two concentrations (0.8 mM and 2.0 mM) of supramolecular hydrogels **SQ/10SQ-DT** were prepared and left to stand overnight before use. The hydrogel samples prior to UV irradiation were separately pipetted into quartz capillaries (2.0 mm) and SAXS measurements were performed. After that, the samples were directly irradiated with UV light (~10.0 mW/cm^2, 365 nm) for 5 min on the quartz capillaries.

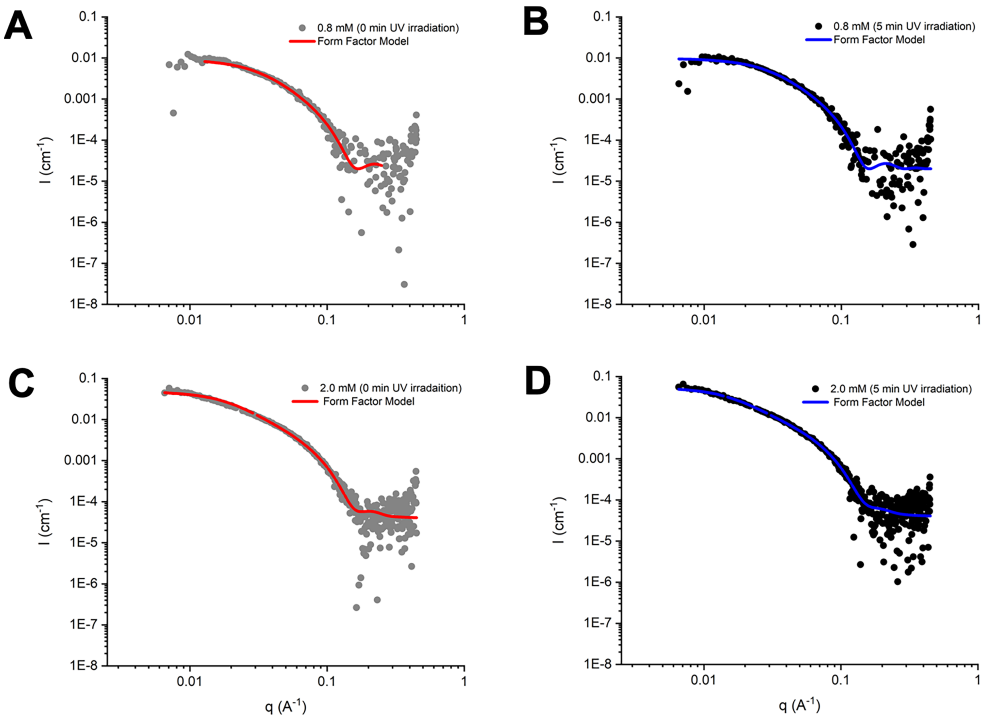

Figure S3.15 Small-angle X-ray scatting profiles of supramolecular hydrogels **SQ/10SQ-DT**: (A) hydrogel concentration of 0.8 mM without UV irradiation; (B) hydrogel concentration of 0.8 mM with 5 min UV irradiation; (C) hydrogel concentration of 2.0 mM without UV irradiation; and (D) hydrogel concentration of 2.0 mM with 5 min UV irradiation. Dots: experimental data; lines: fit a form factor model of a flexible cylinder.

3.6.8 Spatiotemporal photopatterning of bioactive cues

Preparation of custom well inserts

All photopatterning and cell encapsulation experiments (without highlight) were performed in small custom-made well inserts placed inside larger imaging dishes (uncoated 35 mm dishes or uncoated µ-slide 4 well plates) or on top of microscopy slides (#1.5, 30 mm). This strategy facilitated using smaller quantities of hydrogel (~ 30 µL) inside a relatively large (500-2000 µL) liquid reservoir, which enabled easy medium refreshment during hydrogel encapsulated cell culture, or PBS washing in the case of photopatterning experiments.

Briefly, the well inserts were cut from polydimethylsiloxane (PDMS) sheets produced on silicon wafers. A silicon wafer was first silanized by chemical vapor deposition of 1H,1H,2H,2H-perfluorooctyltrichlorosilane under vacuum for

one hour to ensure a proper PDMS detachment later. The pre-crosslinked PDMS (mixed with the curing agent under 1:10) was spin-coated on top of a silicon wafer to ensure a constant height. The PDMS on the wafer was put under vacuum (50 mbar) to degas. After baking at 100 °C for 6 hours, the custom wells were cut, washed with 70% ethanol, dried, and placed inside the designed plate. To increase the surface hydrophilicity of both the cell culture chamber and PDMS inset, the imaging chamber was exposed to UV-Ozone surface treatment for 30 min before use.

Preparation of hydrogel and fluorescein RGD peptide mixtures

To study and visualize the patterning of bioactive cues in the hydrogel through their chemical crosslinking, a fluorescent RGD peptide (**(Fluorescein)GK(DT)GGGRGDS**) was synthesized and hydrogel mixture was first prepared. After sonication in an ice bath, the pre-gel precursor solution of **SQ/10SQ-DT** (6.66 mM, 135 µL) was mixed with different concentrations of the fluorescent RGD peptide (0.01 mM, 0.05 mM and 0.1 mM, 15 µL) by gentle pipetting (10 times). The obtained hydrogel and peptide mixtures were incubated at 37 °C for 15 min to trigger gel formation and further let to equilibrate overnight at room temperature prior to use for photopatterning. All photoactive samples were shielded from light during preparation and subsequent experiments. Finally, the equilibrated hydrogel mixtures, containing **SQ/10SQ-DT** (6.0 mM) and **(Fluorescein)GK(DT)GGGRGDS** (0.01 mM) were then used for photopatterning by application of either a photomask or direct laser writing.

To further calibrate the degree of crosslinking in the photopatterning experiments, homogenous UV irradiation of the hydrogel mixtures containing different known concentrations of **(Fluorescein)GK(DT)GGGRGDS** (e.g., 1.0 µM, 5.0 µM and 10.0 µM) were used.

Photo-patterning through a photomask

The pre-prepared hydrogel and fluorescent RGD peptide mixture (6.0 mM **SQ/10SQ-DT** with 0.01 mM **(Fluorescein)GK(DT)GGGRGDS**, 30 µL) was pipetted into the well insert inside the µ-slide 4 well plate and irradiated with UV light under a photomask (250 µm stripes) through a benchtop LED source (5 min, ~10.0 mW/cm^2, 375 nm). To wash out the unbound fluorescent RGD peptide, the hydrogels were submerged in PBS (800 µL) and incubated at 37 °C. In the first 4 h,

the PBS was changed every hour. The samples were then incubated overnight at 37 °C before imaging.

Two-photon crosslinking using direct laser writing (DLW)

Identical to the photo-patterning experiments using a photomask, the fluorescent RGD peptide and hydrogel mixture (6.0 mM **SQ/10SQ-DT** with 0.01 mM **(Fluorescein)GK(DT)GGGRGDS** was pipetted (30 µL) into custom cut PDMS well insert placed on glass microscope coverslips (#1.5, 30 mm). To keep the hydrogel submerged in PBS during the writing process, a second of the higher PDMS well insert was placed on top of the first insert (with the gel inside). Finally, the two-stage PDMS well insert (30 µL reservoir 1 with hydrogel, 100 µL reservoir 2 with PBS inside), was sealed with a second glass coverslip to prevent evaporation.

Two-photon crosslinking, by direct laser writing (DLW) was performed using the Photonics Professional GT. 3D structures were designed in Autodesk Inventor and converted to the stereolithography file format (STL). Then, STL files were imported into DeScribe to obtain a suitable mesh for DLW. The hydrogel and crosslinker composite were exposed to a 780 nm laser (Ti-Sapphire, 20 mW maximum at sample surface) using a 20x Air objective. In the x, y-directions the DLW mesh was scanned by the laser through galvanic mirrors, and then stitched, slice-by-slice, in the z-direction with a piezo stage. The scanning speed was set at 250 µm/s with a power scaling of 1.00. All DLW procedures were performed under yellow light (λ = 577-597 nm) to prevent spontaneous cross-linking during the writing process. The samples were washed with PBS (5 times) and kept in PBS at room temperature overnight before imaging.

Confocal imaging of photo-patterned hydrogels

The photo-patterned hydrogels were imaged using a 10x and 20x objective on a Nikon Eclipse Ti microscope equipped with a Yokogawa confocal spinning disk unit operated at 10,000 rpm. The attached fluorescein was excited with a 0.2 mW, 488 nm laser light from solid state diode laser supported in an Agilent MLC4 unit. Images were captured using an exposure time of 200-300 ms by an Andor iXon Ultra 897 high speed EM-CCD camera. The acquired fluorescent images were background corrected to visualize the fluorescent RGD crosslinking.

Quantification of degree of photo-patterned RGD peptide within the hydrogel

The fraction of **DT-RGD** peptide bound to the hydrogel can be quantified using the fluorescent RGD peptide (**(fluorescein)GK(DT)GGGRGDS**). The emission intensity of hydrogel mixtures upon laser excitation is directly proportional to the concentration of fluorescein present. Therefore, samples with different known concentrations and homogenous UV illumination were used to calibrate and estimate the fraction of **DT-RGD** bound in photopatterning experiments.

The fluorescent emission of the patterned hydrogel, acquired by spinning-disk confocal microscopy, was measured for two objectives (10x NA 0.3, and 20x NA 0.75) across a wide range of 488 nm excitation intensities (laser power) for two different samples at a fluorescent RGD peptide concentration of 10.0 μM (**Figure S3.16A**). To assist in later calibrations, a quadratic fit (with degree fixed at 0) was done to inter- and extrapolate the intensity of fluorescent emission as a function of laser power. Next to different laser powers, the effect of varying concentrations of fluorescein versus emission intensity was also measured (**Figure S3.16B**) for each objective and laser power. The fluorescent emission was found to be linearly proportional to the concentration. All intensities shown are averaged intensities over a block of 100 x 100 pixels in the center of the field-of-view (512 x 512) of the camera.

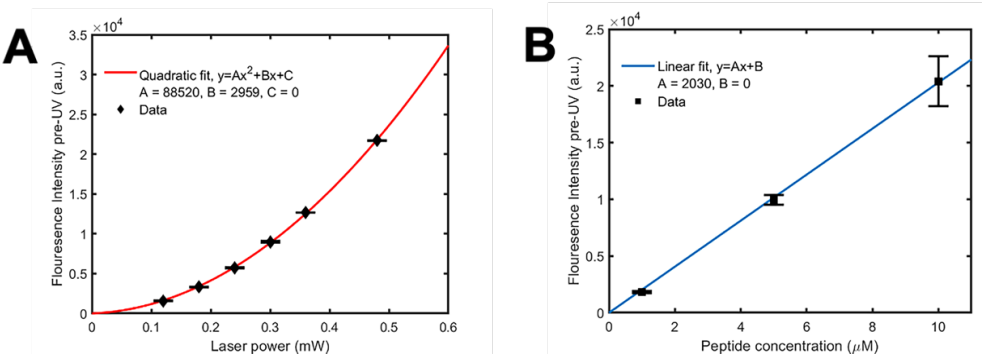

Figure S3.16 Calibration results of the mixtures of hydrogel **SQ/10SQ-DT** (6.0 mM) with different concentrations of fluorescent RGD peptide (**(fluorescein)GK(DT)GGGRGDS**) (1.0 µM, 5.0 µM and 10.0 µM) in the unbound state. (A) Fluorescent emission intensity of hydrogel containing fluorescent RGD peptide (10.0 µM) before UV exposure as a function of the laser power (excitation intensity) using a 10x objective. A quadratic fit (C = 0) was used to inter- and extrapolate intensities of other laser powers. (B) Fluorescent emission intensity of fluorescent RGD peptide before UV exposure as a function of its concentration (1.0 µM, 5.0 µM and 10.0 µM). A linear fit (B = 0) was used to inter- and extrapolate intensities of different concentrations. Error bars are standard deviations over measurements performed.

After the calibration measurements, the mixture of hydrogel and fluorescent RGD peptide samples were homogeneously irradiated with UV light for 5 min using a benchtop LED (~10 mW/cm^2, 375 nm). Subsequently, the samples were covered with PBS to wash out the unbound peptide. The samples were imaged after washing for 4 h and after further washing for 24 h. During the first 4 h washing period, the samples were changed with fresh PBS each hour. The emission intensities of the samples before (*black line*) and after UV irradiation (*red line*) was shown in **Figure S3.17**. All normalized intensities were separately scaled (**Figure S3.17**) using the intensity measured before UV irradiation for each concentration respectively (**Figure S3.16B**). The fraction of fluorescent RGD peptide bound was 0.2 for all measured concentrations. This means that the yield of photopatterned induced crosslinking is directly proportional to the concentration used when homogenous UV irradiation is applied. Further, extensive washing for a longer time (24 h) did not influence the retention of fluorescent RGD peptide (**Figure S3.17**, *green line*).

Using the calibration experiments shown above, the retention of fluorescent RGD peptide within the patterned hydrogels was estimated. The 10x objective (**Figure S3.16** and **Figure S3.17**) was used to collect the calibration data from the photomask samples, and the 20x objective (data not shown) for the DLW patterning samples. In both cases, the mixture of **SQ/10SQ-DT** (6.0 mM) hydrogel

and fluorescent RGD peptide (1.0 μM) was explored. And the calibration experiment was used to relate the intensity imaged to the concentration of RGD present. These samples were imaged at a laser power of 1.44 mW. The estimated concentration of fluorescent RGD peptide bound was shown in **Figure 3.4B** for the photomask and **Figure S3.18** for the DLW assay.

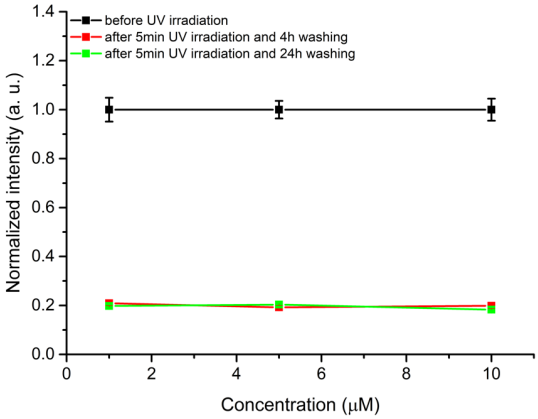

Figure S3.17 Normalized fluorescein intensity of multicomponent hydrogel **SQ/10SQ-DT** (6.0 mM) containing different concentrations of fluorescent RGD peptide (**(fluorescein)GK(DT)GGGRGDS**) (1.0 μM, 5.0 μM and 10.0 μM) before and after 5 min UV irradiation using a benchtop LED source (~10.0 mW/cm^2, 375 nm), and further washing with PBS for 4 h and 24 h. The intensity of each sample after UV irradiation was separately normalized to its value of fluorescence intensity before UV irradiation. Error bars are standard deviations over measurements performed.

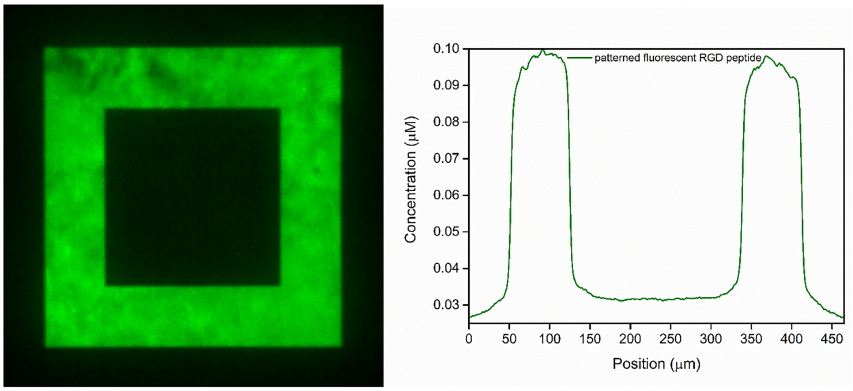

Figure S3.18 2D confocal fluorescence images of fluorescent RGD peptide (**(Fluorescein)GK(DT)GGGRGDS**) patterned within hydrogel via direct-laser writing (DLW) and the coupled RGD concentration varied with the position of the patterned and un-patterned area.

3.6.9 Cell culture and lentiviral transduction

Cell culture

NIH 3T3 and C2C12 cell lines were cultured and maintained in DMEM medium-high glucose (D6546) with 10% fetal bovine serum (FBS), 1% Glutamax, 0.2% penicillin and streptomycin. The Hs578T cell line was culture in RPMI 1640 medium with 10% FBS, 0.2% penicillin and streptomycin. All the cells were cultured in an incubator at 37 °C with a 5% CO_2 atmosphere and kept below 70% confluency.

Generation of stable mCherry-LifeAct reporter cell lines

For visualization of the actin cytoskeleton, C2C12 and Hs578T WT cells were transduced using a lentiviral mCherry-LifeAct cDNA expression vector (provided by Dr. Olivier Pertz, University of Basel, Basel, Switzerland), and were further cultured in a selection medium containing 2 μg/ml puromycin in an incubator at 37 °C with a 5% CO_2 atmosphere.

3.6.10 3D cell encapsulation and cell viability assay

Cells were first dissociated from T-25 culture flasks (< 12 passages) through treatment with 0.25% trypsin for NIH 3T3 and Hs 578T cells, and 0.25% trypsin-EDTA solution for C2C12 cells. The resulting cell suspensions were centrifuged, and then re-suspended in fresh medium. Then the obtained single cell suspensions (3.0×10^6 - 8.0×10^6 cells/mL, 15 μL) were separately mixed with the pre-prepared hydrogel **SQ/10SQ-DT** (4.44 mM, 135 μL) in PBS by gently pipetting up and down (~10 times) to obtain a homogeneous cell-laden hydrogel (4.0 mM **SQ/10SQ-DT**, 3.0×10^5 - 8.0×10^5 cells/mL cell density). The cell-laden hydrogels (12 μL) were pipetted into a μ-slide 15 well plate and equilibrated for 5 min in an incubator at 37 °C to recover the initial gel state. The cell-laden hydrogels were then left without UV light irradiation, or further stiffened using UV light from a benchtop LED source (5 min, ~10 mW/cm^2, 375 nm). The cell culture media (48 μL) was carefully layered on top of the hydrogels and placed in an incubator at 37 °C.

Cell viability was measured after 24 h using LIVE/DEAD (calcein AM/propidium iodide (PI)) staining. Prior to staining, the medium was carefully removed from the top of the hydrogel, and washed with PBS (2 x 48 μL). The staining solution (48 μL) containing calcein AM (2.0 μM) and PI (1.5 μM) was

pipetted on top of the hydrogel and incubated at 37 °C for 30 min. Then, the remaining staining solution was removed, and further washed with PBS (2 x 48 µL). Additional PBS (48 µL) was added on top of the hydrogel to avoid the hydrogel drying during imaging.

The stained cell-laden hydrogels were imaged on a Zeiss LSM 710 confocal laser scanning microscope equipped with a Zeiss 5× objective. Fluorescent Z-stack images (37-44 images/per sample) through the gel were acquired at a resolution of 512 x 512 pixels (0.69 um/pix) using an excitation wavelength of 488 nm and an emission filter of 519-582 nm for calcein AM, and an excitation wavelength of 532 nm and an emission filter of 615-695 nm for PI. The percentage of cell viability was determined by counting the viable (*green*) cells with calcein AM staining and dead (*red*) cells with PI-staining using Image J.

3.6.11 Morphology study of C2C12 encapsulated in various hydrogels

C2C12 morphology in uniform peptide patterned hydrogels

To obtain uniform peptide-functionalized supramolecular hydrogel, the pre-gel precursor solution (after sonication in ice water) **SQ/10SQ-DT** (3.7 mM, 135 µL) was separately mixed with cell-adhesion peptide **DT-RGD** (4.44 mM, 15 µL) or the scrambled peptide **DT-DGR** (4.44 mM, 15 µL) by gentle pipetting (~10 times). This resulted in a final solution containing **SQ/10SQ-DT** (3.33 mM) and containing **DT-RGD** (0.44 mM) or **DT-DGR** (0.44 mM). Hydrogels were formed after 15 min incubating at 37 °C, and left to equilibrate overnight at room temperature prior to further usage.

To seed the cells in supramolecular hydrogels, the pre-made supramolecular gels above (135 µL) were mixed with a C2C12 cell suspension (5.0 x 10^6 cells/mL, 15 µL) by gentle pipetting (~10 times), and then incubated at 37 °C for 15 min. The final cell-laden hydrogels consisted of a cell density (5.0 x 10^5 cells/mL) and hydrogel **SQ/10SQ-DT** (3.0 mM) with **DT-RGD** or **DT-DGR** (0.4 mM). The obtained final mixture (12 µL) was then pipetted into a µ-slide 15 well plate and left to stand in the incubator at 37 °C for 5 min. Then, the cell-laden hydrogels were irradiated with UV light for different times (0 min and 5 min) using a benchtop LED source (~10 mW/cm^2, 375 nm). Cell culture media (48 µL) was layered on top of the hydrogels, and cultured in an incubator at 37 °C until further usage. Cell culture media was refreshed every two hours during the first 6 h, to

wash out the uncoupled **DT-RGD** or **DT-DGR** after UV irradiation. During the following culture, media was replaced every day.

At day 3, cell viability and morphology were measured by confocal laser scanning microscopy after staining with calcein AM/propidium iodide (PI) as described in section **3.6.10**.

C2C12 morphology in photo-patterned RGD hydrogels

Photopatterned samples were prepared similarly to the uniform RGD functionalized gels as mentioned above, with the addition of the fluorescent RGD peptide **(Fluorescein)GK(DT)GGGRGDS** (1.0 μM) into the gel/**DT-RGD** mixture, but maintaining the same total RGD concentration (0.4 mM). The fluorescent RGD peptide here was added to visualize the RGD photo-patterned areas. Pre-made cell-hydrogels were pipetted into a μ-slide 4 well plate with custom made PDMS well insets (produced as described in **3.6.8**) and then irradiated with UV light for 5 min in the presence of a photomask (250 mm stripes) using a benchtop LED source (~10 mW/cm^2, 375 nm). The cell-hydrogels were submersed in culture media (800 μL) and refreshed every hour during the first 4 hours of incubation to wash out unbound **DT-RGD** and **(Fluorescein)GK(DT)GGGRGDS**. Finally, the samples were left to incubate at 37 °C under a 5% CO_2 atmosphere until further study. During culture, media was replaced every day.

At day 3, immunostaining of C2C12 cells in photopatterned hydrogels was performed. First, the samples were fixed with 4% paraformaldehyde solution in PBS (800 μL) at room temperature for 30 min. The samples were then washed with PBS (4 x 800 μL), followed by cell membrane permeabilization using 0.1% TritonX-100 solution in PBS (800 μL) at room temperature for 2 h. Samples were washed with PBS (4 x 800 μL) and non-specific protein interactions were blocked using 2% bovine serum albumin (BSA) (800 μL) at room temperature for 2h. Samples were washed with PBS (4 x 800 μL) and then F-actin stained using AlexaFluor488-phalloidin antibody (1:300) in 0.1% BSA overnight at 4 °C. Finally, the samples were further washed with PBS (4 x 800 μL). The stained samples were covered with fresh PBS and stored at 4 °C before imaging.

C2C12 cell morphology in hydrogels containing different RGD concentration

The preparation of 3D C2C12 cell-laden hydrogel **SQ/10SQ-DT** (6.0 mM, total concentration) containing different concentrations of **SQ-RGD** (0 mM; 0.1 mM; 0.2 mM and 0.4 mM) followed the same procedure as shown in **3.6.10**. The

obtained cell-laden hydrogel (12 µL) was gently pipetted into the µ-slide 15 well plate and carefully covered with cell culture medium (48 µL). All the cell-laden hydrogels were maintained in an incubator at 37 °C with a 5% CO_2 atmosphere prior to use. After 24 h culture, the C2C12 was stained with calcein AM/PI and imaged in confocal microscopy to check the cell viability and morphology.

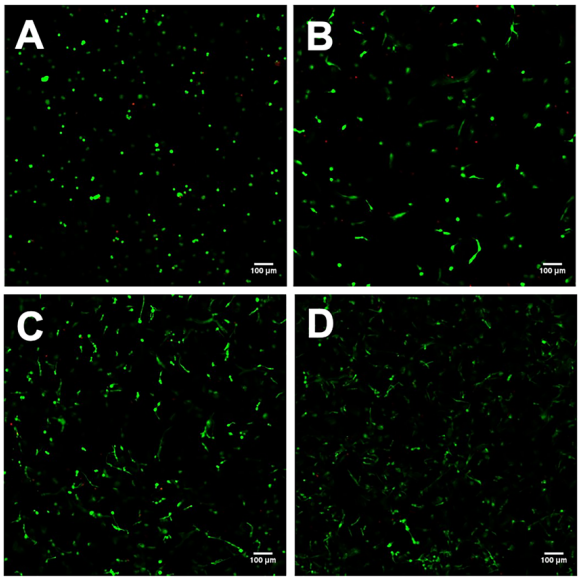

Figure S3.19 Representative confocal microscopy images of C2C12 cells after 24 h culture within hydrogel **SQ/10SQ-DT** (6.0 mM) containing different concentration of **SQ-RGD** prior to UV irradiation: (A) 0 mM; (B) 0.1 mM; (C) 0.2 mM; and (D) 0.4 mM. The C2C12 cells were stained with calcein AM (*green*) for viable cells, and PI (*red*) for dead cells. Scale bar: *100 µm*.

C2C12 cell morphology in hydrogels with varied stiffness

To explore the influence of hydrogel stiffness on cell morphology, mCherry-LifeAct C2C12 (5 x 10^5 cells/mL) cells were encapsulated in 3D in the 6.0 mM **SQ/10SQ-DT/3.4SQ-RGD** hydrogel (namely, containing 0.2 mM **SQ-RGD**) following the procedure in section **3.6.10**. The cell-laden hydrogel (12 µL) was gently pipetted into a µ-slide 15 well plate and was stiffened using UV irradiation for 5 min with a benchtop LED source (~10 mW/cm^2, 375 nm) at day 0 or day 1. A sample was also prepared without UV irradiation as a control. The cell culture medium (48 µL) was layered on top of the hydrogel. The cell-laden hydrogels were then maintained in an incubator at 37 °C with a 5% CO_2 atmosphere prior to use. The cell culture medium was refreshed every day. During the dynamic stiffening process at day 1,

the cell culture medium was carefully removed from the top of the hydrogel by pipetting prior to UV irradiation.

Quantification of cell spreading

An in-house Matlab (Mathworks) code was used to quantify cell spreading, which allowed automated adaption of edge-detection settings for every individual cell recognized. This individual optimization of edge-detection parameters was necessary, as fluorescence intensities and signal-to-noise ratios varied notably per cell. Such variations were primarily due to differences in imaging height of each cell in the gel, but is also attributable to inherent heterogeneity in LifeAct expression.

Before edge detection, all images in every z-stack were preprocessed. First, illumination inhomogeneities in the microscope field of view were flattened using FIJI plugin BaSiC.[4] Then, importing images into the Matlab, followed by setting the appropriate contrast and subtracting the background, the image was despeckled by median filtering and a Gaussian blur was applied. Then edges were determined using the Sobel method (thresholded 0.01-0.1), and subsequently dilated, filled and eroded to find a binary mask for each cell area. The cell-edge was defined as the perimeter of pixels at the boundary of the cell area in the binary mask. Using the binary mask, the centroid (center of mass), area (A), perimeter (P), total skeleton length (S) and ferret-diameters (F_{min} and F_{max}) were calculated using the appropriate scale (0.68 µm/pix).

For every cell recognized, the pixel intensities of an area larger, and around those cells was extracted from the original images and saved in a database. Thereby a library of small and single cell images was created. By comparing the centroids (in pixel number) of all recognized cells across all the different z-slices, edges belonging to the same cell were identified as a single cell and their pixels linked to create single cell z-stacks. These single cell (mini) z-stack images were then, one-by-one, automatically presented to the user via a graphical-user-interface with the option to adjust detection parameters to best determine the cell edge, and the choice of selecting the appropriate z-slice, and to find the maximum spread. This means that every cell analyzed was manually checked for correct edge-recognition, thereby eliminating any chance of erroneous detection due to highly varied fluorescence intensities. This cycle can be repeated multiple times with different starting parameters, allowing all detectable cells to be added to the dataset.

For each experimental condition, the full distributions of each observable measured was shown in **Figure 3.5** and **Figure S3.20**, and their mean was displayed in **Tables S3.2-3.4**. The circularity (C) and aspect ratio (AR) are calculated by $C = 4*pi*A/P^2$ and $AR = F_{min}/F_{max}$. The error estimates in **Table S3.2-3.4** were the 95% confidence intervals of the mean. All cell edges of touching cells or those in close proximity (± 50 μm) to each other were discarded.

Table S3.2 Summary of quantitative analyses of the C2C12 cells after 3 days culture within the supramolecular hydrogel (3.0 mM **SQ/10SQ-DT**) in 3D containing 0.4 mM **DT-RGD** and the fluorescent RGD peptide photopatterned using a photomask (200 μm stripes) under UV light using a benchtop LED source (~10 mW/cm^2, 375 nm) for 5 min.

Parameters	RGD patterned areas (*green*)	RGD unpatterned areas (*black*)
Area (μm^2)	657 ± 27	568 ± 38
Perimeter (μm)	108 ± 4	92 ± 5
Circularity	0.805 ± 0.019	0.906 ± 0.023
Skeleton Branch Length (μm)	23 ± 2	22 ± 3

Table S3.3 Summary of quantitative analyses of the mCherry-LifeAct C2C12 cells after encapsulation within the supramolecular hydrogel (6.0 mM **SQ/10SQ-DT/3.4SQ-RGD**) in 3D and the application of different UV light irradiation times (0 min and 5 min) at day 0 or day 1 using a benchtop LED source (~10 mW/cm^2, 375 nm).

Parameters	After 1 day of culture in hydrogel (0 min UV irradiation)	After 1 day of culture in hydrogel (5 min UV irradiation at day 0)	After 3 days of culture in hydrogel (0 min UV irradiation)	After 3 days of culture in hydrogel (5 min UV irradiation at day 1)
Area (μm^2)	743 ± 83	407 ± 29	1054 ± 89	1021 ± 85
Perimeter (μm)	186 ± 19	99 ± 8	220 ± 18	234 ± 17
Circularity	0.414 ± 0.043	0.69 ± 0.054	0.436 ± 0.041	0.365 ± 0.034
Skeleton Branch Length (μm)	64 ± 8	29 ± 5	84 ± 9	89 ± 9
Max Feret diameter (μm)	67 ± 6	37 ± 3	76 ± 6	80 ± 5
Min Feret diameter (μm)	29 ± 3	21 ± 1	32 ± 2	34 ± 2
Aspect ratio	0.504 ± 0.031	0.642 ± 0.034	0.494 ± 0.025	0.471 ± 0.022

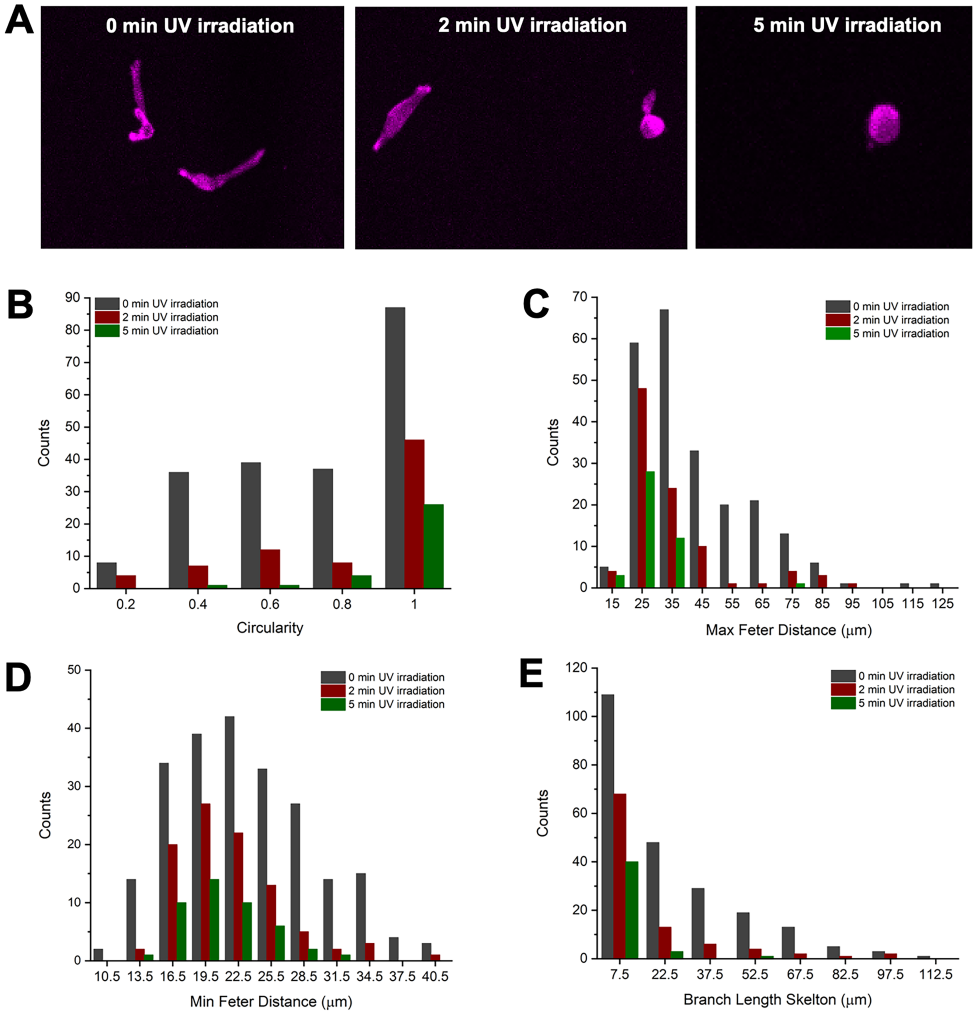

Figure S3.20 Encapsulation of the mCherry-LifeAct Hs587T breast cancer cells in 3D within supramolecular hydrogel (4.0 mM **SQ/10SQ-DT/10SQ-RGD**) and the application of UV light with different irradiation times (0 min, 2 min and 5 min) using a benchtop LED source (~10 mW/cm^2, 375 nm) and cultured afterwards for 3 days: (A) Representative confocal images; and the calculated distribution of the (B) Circularity; (C) Max Feret Diameter; (D) Min Feter Diameter and (E) Branch length Skelton.

Table S3.4 Summary of quantitative analyses of the mCherry-LifeAct Hs587T breast cancer cells after encapsulation within the supramolecular hydrogel (4.0 mM **SQ/10SQ-DT/10SQ-RGD**) in 3D and irradiation with UV light (0 min, 2 min and 5 min) using a benchtop LED source (~10 mW/cm^2, 375 nm) and after culture for 3 days.

Parameters	0 min UV irradiation	2 min UV irradiation	5 min UV irradiation
Area (µm^2)	614 ± 32	494 ± 43	413 ± 35
Perimeter (µm)	104 ± 5	87 ± 6	72 ± 5
Circularity	0.799 ± 0.03	0.899 ± 0.045	1.016 ± 0.038
Skeleton Branch Length (µm)	23 ± 3	15 ± 3	6 ± 2
Max Feret diameter (µm)	42 ± 2	35 ± 3	28 ± 2
Min Feret diameter (µm)	23 ± 1	22 ± 1	21 ± 1

3.6.12 mCherry-LifeAct Hs578T cell migration in supramolecular hydrogels

3D cell encapsulation for migration study

To obtain the 3D cell-laden hydrogels for the migration study, mCherry-LifeAct Hs587t cells were encapsulated into the supramolecular hydrogel (4.0 mM **SQ/10SQ-DT/10SQ-RGD**) following the same procedure as mentioned above (see **3.6.10**). The varied stiffness of the hydrogel was obtained with different light irradiation times (e.g., 0 min or 5 min) using a benchtop LED (~10 mW/cm^2, 375 nm). Moreover, the hydrogel could be stiffened at the user demand time point, for example, day 0 or day 2 after seeding.

Imaging and analysis of cell migration

Samples were imaged using a 10x NA 0.3 objective on a confocal spinning-disk microscope. The mCherry-LifeAct Hs587T cells were imaged every 5 min over total 16 hours using an exposure time of 200 ms. The fluorophore was excited using a 561 nm laser at 2.6 mW. For each sample, 1-8 positions with the volume slices (701 x 701 x 160 µm) were chosen and were imaged using z-stacks at a scan speed of 10 µm/step. To investigate the influence of temporal stiffening of the hydrogel

on cell migration, the time lase images of the samples in the same position before and after UV irradiation were also collected.

In order to create a two-dimensional time-series of cell motion, the image stacks were maximally z-projected at every position using ImageJ (http://imagej.nih.gov/ij/). Then the images were binarized by intensity thresholding and contrast adjustment. To determine the x, y-coordinates of the center-of-mass of each cell in each frame, cell evaluator plugin[5] in ImageJ was used. By linking all these x, y-positions together, cell trajectories were obtained and plotted in **Figure 3.8**.

The trajectories with an in-house Matlab (version 2019b, The Mathworks) code were analyzed. The 2D-projected instantaneous velocity was used to characterize the migratory activity of the cells and the MSD was a measure of the total space explored by the cell over time. The calculated instantaneous velocities and MSD of cell trajectories, before and after hydrogel stiffening, were shown in **Figure 3.8C, D**. Finally, the maximal displacement (with respect to the origin) of the cells during the time-lapse was calculated, which was a measure of the distance explored by the moving cell (**Figure 3.8**).

3.6.13 References

(1) Tong, C.; Liu, T.; Saez Talens, V.; Noteborn, W. E. M.; Sharp, T. H.; Hendrix, M.; Voets, I. K.; Mummery, C. L.; Orlova, V. V.; Kieltyka, R. E. *Biomacromolecules* **2018**, *19* (4), 1091-1099.

(2) Tong, C.; Wondergem, J. A. J.; Heinrich, D.; Kieltyka, R. E. *ACS Macro Lett.* **2020**, *9* (6), 882-888.

(3) Yu, H.; Wang, Y.; Yang, H.; Peng, K.; Zhang, X. *J. Mater. Chem. B* **2017**, *5* (22), 4121-4127.

(4) Peng, T.; Thorn, K.; Schroeder, T.; Wang, L.; Theis, F. J.; Marr, C.; Navab, N. *Nat. Commun.* **2017**, *8* (1), 1-7.

(5) Youssef, S.; Gude, S.; Radler, J. O. *Integr. Biol.* **2011**, *3* (11), 1095-1101.